REPORT DOCUMENTATION PAGE

Form Approved
OMB NO. 0704-0188

1. AGENCY USE ONLY *(Leave blank)*	2. REPORT DATE	3. REPORT TYPE AND DATES COVERED
		Final 23 Jan 95 - 22 Jan 96

4. TITLE AND SUBTITLE

Instrumentation for Advanced Feedback Control of a Metalorganic Chemical Vapor Deposition Facility

5. FUNDING NUMBERS

DAAH04-95-1-0061

6. AUTHOR(S)

R.S. Smith, S.P. DenBaars, and M.S. Gaffney

7. PERFORMING ORGANIZATION NAMES(S) AND ADDRESS(ES)

Office of Research
University of California,
Santa Barbara, CA 93106

9. SPONSORING / MONITORING AGENCY NAME(S) AND ADDRESS(ES)

U.S. Army Research Office
P.O. Box 12211
Research Triangle Park, NC 27709-2211

10. SPONSORING / MONITORING AGENCY REPORT NUMBER

ARO 34356.1-RT-RIP

11. SUPPLEMENTARY NOTES

The views, opinions and/or findings contained in this report are those of the author(s) and should not be construed as an official Department of the Army position, policy or decision, unless so designated by other documentation.

12a. DISTRIBUTION / AVAILABILITY STATEMENT

Approved for public release; distribution unlimited.

12 b. DISTRIBUTION CODE

13. ABSTRACT *(Maximum 200 words)*

This report describes the purchase of equipment for instrumentation and feedback control of chemical vapor deposition reactors for III-V compound semiconductor device manufacturing. A combination of ultrasonic and optical sensors are used to measure component gas concentrations and the growth rate at the sample surface. Mass flow controllers, at various locations in the reactor gas delivery system, are used to control the pure component flow. Two optical sensing systems are being developed with funds from this grant. The first is an ultraviolet light absorption monitor, which uses the absorption at a particular ultraviolet frequency to measure the gas partial pressure, and thereby infer the concentration above the growing surface. The second is a reflective difference spectroscopy system which determines the growing layer thickness in real-time, from the polarization of a reflected light beam. Digital computers are used to implement the data acquisition and feedback control systems.

The report contains an overview of the metalorganic chemical vapor deposition system. The sensing, actuation, and control approaches are described in detail. A complete description of the components is also provided. The research is ongoing and the publications related to the funded development work are attached.

14. SUBJECT TERMS

Metalorganic Chemical Vapor Deposition Reactors
Semiconductor Manufacturing, Process Control, Feedback Control

15. NUMBER IF PAGES

78

16. PRICE CODE

17. SECURITY CLASSIFICATION OR REPORT	18. SECURITY CLASSIFICATION OF THIS PAGE	19. SECURITY CLASSIFICATION OF ABSTRACT	20. LIMITATION OF ABSTRACT
UNCLASSIFIED	UNCLASSIFIED	UNCLASSIFIED	UL

DISCLAIMER NOTICE

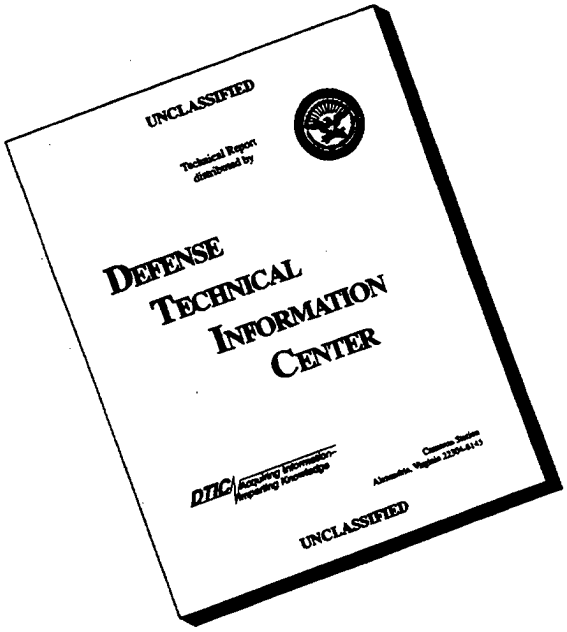

THIS DOCUMENT IS BEST QUALITY AVAILABLE. THE COPY FURNISHED TO DTIC CONTAINED A SIGNIFICANT NUMBER OF PAGES WHICH DO NOT REPRODUCE LEGIBLY.

Instrumentation for Advanced Feedback Control of a Metalorganic Chemical Vapor Deposition Facility

Final Progress Report

R. S. Smith
S. P. DenBaars
M. S. Gaffney

June 17, 1996

Advanced Research Projects Agency
Grant monitored by: U.S. Army Research Office

DAAH04-95-1-0061

University of California, Santa Barbara

Abstract

This report describes the purchase of equipment for instrumentation and feedback control of chemical vapor deposition reactors for III-V compound semiconductor device manufacturing. A combination of ultrasonic and optical sensors are used to measure component gas concentrations and the growth rate at the sample surface. Mass flow controllers, at various locations in the reactor gas delivery system, are used to control the pure component flow. Two optical sensing systems are being developed with funds from this grant. The first is an ultraviolet light absorption monitor, which uses the absorption at a particular ultraviolet frequency to measure the gas partial pressure, and thereby infer the concentration above the growing surface. The second is a reflective difference spectroscopy system which determines the growing layer thickness in real-time, from the polarization of a reflected light beam. Digital computers are used to implement the data acquisition and feedback control systems.

The report contains an overview of the metalorganic chemical vapor deposition system. The sensing, actuation, and control approaches are described in detail. A complete description of the components is also provided. The research is ongoing and the publications related to the funded development work are attached.

Contents

1 Problem Statement

In the past few years, metalorganic chemical vapor deposition (MOCVD) has emerged as one the most promising technique for production of the next generation of high speed electronic and opto-electronic devices. However, the MOCVD technique currently suffers from lack of *in situ* process control which causes a lack of precise reproducibility. Precise control of the composition and growth rates will allow the construction of numerous high performance III-V semiconductor devices. This precision can be improved by applying feedback control to the MOCVD process. Issues that arise during the application of feedback control to MOCVD include, developing real-time feedback monitors, generating a system model, defining the control loops - both sensors and actuators, and then designing the controllers. Further challenges arise in measuring the controller performance, such as designing growth structures that can provide specific composition and thickness information with post-growth evaluation techniques.

2 Project Description

2.1 Introduction

This project is a collaborative effort which applies control theory to the processing of electronic materials. Because these processes are typically run in an open loop fashion, there is much room for improvement by applying feedback control. We are investigating closed loop control of the MOCVD process. The purpose of this work is to greatly reduce the high degree of process variance, which will improve MOCVD process yields and also enable fabrication of complex devices. Specifically, real-time control of the MOCVD will address both layer-to-layer, and run-to-run reproducibility, as well as lateral sample uniformity. In addition, this work will generate a better understanding of the MOCVD process dynamics and disturbances that hinder tolerances, resulting in improved MOCVD machine design and growth procedures.

Applying control theory to the processing of electronic materials at UCSB requires a strong collaborative effort from members of the Center fo Control Engineering and Computation in the Department of Electrical and Computer Engineering, with compound semiconductor researchers in the Department of Materials. The application of control to semiconductor processes is an new field where control researchers are just starting to venture. These processes have a lot to gain from control theory because they are currently run in an open loop fashion. Calibrations and adjustments are made before a run or by an operator during a run. By monitoring the process in real time, these adjustments can be made automatically and with extreme precision.

Section 2 of this report begins with a brief review of the MOCVD process, followed by a discussion on the motivation for feedback control. Then, the control strategy and status

are summarized. Section 2 is concluded with a more detailed description of the control applications. Section 3 contains a brief list of the equipment budget, followed by a more detailed description of every item purchased for instrumentation and feedback control of the MOCVD system. This research and its impact are summarized in Section 4. The appendix contains a list of scientific personnel who have benefited from this grant while working towards advanced degrees, as well as copies of the four publications that have been generated from the project thus far.

2.2 The MOCVD Process

The following description is a brief summary of the system overview contained in [1, 2]. An example of ternary MOCVD growth is when two column III alkyl sources, such as trimethylgallium (TMG) and trimethylindium (TMI), are mixed in a vapor phase with an organometallic column V source, such as tertiarybutylarsine (TBA). Under specific conditions, including reactor pressure, temperature, and molar flow rates, the deposition of a solid will occur. For TMG, TMI, and TBA, the resulting solid is $Ga_xIn_{(1-x)}As$. In III-V growth, the column III and V atoms primarily deposit in a 1:1 ratio. The column III ratio x, in the ternary compound example, is one of two main parameters to control. This molar ratio, or composition, has tolerances of $\pm$ 0.01 in order to obtain the desired emission wavelength from a quantum-well laser for example. The thickness or growth rate is the other parameter which must obtained precisely in the fabrication of electronic-grade devices.

Figure 1 is an overview of the gas flow through the system for a single source. The source chemicals are transported to the growth chamber in a vapor phase by bubbling hydrogen gas through the source vessel that stores the liquid reagent. This vessel is referred to as a bubbler. The resulting gas flow from the bubbler consists of hydrogen and the desired concentration of the source. The source concentration is regulated by three mass flow controllers, the input controller located before the bubbler (input MFC), an H_2 dilution controller located after the bubbler (dilution MFC), and the last one located before the injection manifold (injection MFC) and a pressure controller (bubbler PCV).

The separate gases are mixed in an injection manifold, then sent to the growth chamber to thermally decompose onto the substrate. A fast switching manifold prevents dead spaces and the premature component reactions, leading to interfaces with the desired abruptness. Gas molecules in the chamber diffuse through a stagnant layer to the substrate which then decompose on the surface. Products of the decomposition move over the surface until they find available lattice sites where they are incorporated into the lattice [3, p. 135]. The susceptor is under tight temperature control (via IR lamps) to provide uniform film composition and thickness across the substrate. For the desired crystal growth to occur, the column III reagent compositions sent to the reactor are precise quantities, while the column V compositions are present in an overabundance. After a growth, information about the resulting composition and thicknesses can be

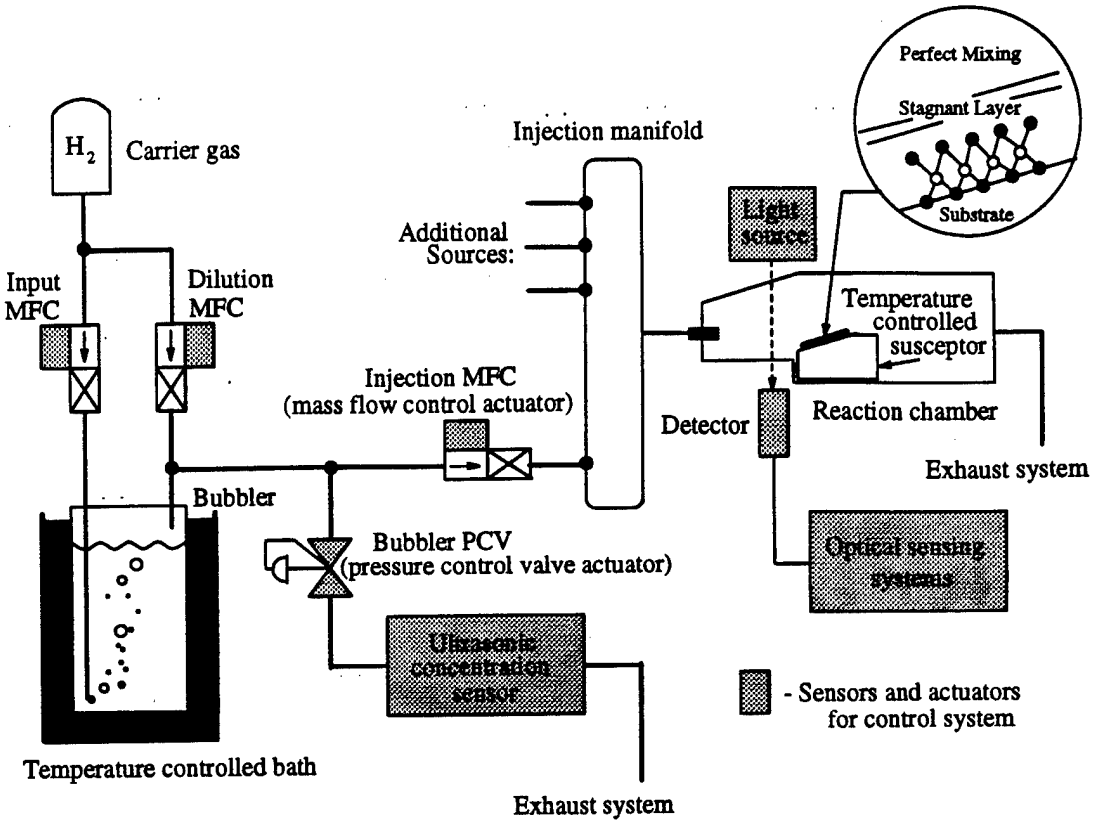

Figure 1: Simplified schematic overview of the MOCVD process for one gas. The available sensors and actuators for control are shown by the grey shading.

determined using X-ray diffraction techniques.

In mass-transport limited MOCVD processes, both composition and growth rate (thickness) are proportional to the delivery rate of the column III precursors. The key parameter is the pure component flow rate, which is the product of the concentration of the source in the hydrogen carrier multiplied by the total flow rate of the source in the carrier. The typical growth procedure involves measuring the concentration of the ultrasonic concentration monitor (shown in Figure 1) before growth, and then adjusting the mass flow controller located just before the injection manifold (injection MFC) so that the product of the concentration and flow rate is the desired pure component flow rate. During growth however, the mass flow controller set point is not adjusted. Consequently, concentration disturbances with time constants faster than a growth period can corrupt the target composition and thickness.

Feedback control systems require both sensors, to measure the state of the system and actuators, to modify the state of the system. The available sensors and actuators for the MOCVD process are shown Figure 1 by the grey shading. The available sensors include the ultrasonic concentration monitor (Epison) [4], located upstream in the gas

deliver section, the ultraviolet absorption monitor, located downstream just before the susceptor, and the reflective-difference spectroscopy monitor, also located downstream at the susceptor (these downstream sensors are labeled as *optical sensing systems* in Figure 1).

2.3 Motivation for Control

In [1, 2], a bubbler disturbance was shown to corrupt the pure component flow rate during growth, thereby degrading the desired device composition and thickness. This bubbler disturbance occurs in the gas delivery system and is considered here to be an upstream disturbance. A control loop located in the gas delivery system has been shown to reject these disturbances and significantly improve growth [1, 2, 5]. A key component in the upstream control system was the ultrasonic concentration sensor. Although the upstream disturbances can be sensed and rejected using the ultrasonic concentration sensor, there is evidence of downstream disturbances that cannot be detected by the upstream sensor. One downstream disturbance seen in the growth data is manifested as a gas flow disturbance, and is believed to be caused by pressure fluctuations during an injection manifold switch event. This type of flow disturbance could degrade the desired quality of abrupt interfaces [6]. Hence a control system that can measure and then reject these disturbances is desirable. Additionally, the pure component flow is expected to be disturbed in the downstream system due to the changing temperature gradients along the piping system. Evidence of thermal diffusion that leads to a change in reactant partial pressure is discussed in [7]. The existence of these disturbances motivated the development of additional sensing systems, located downstream from the gas delivery system, at the reaction chamber. Once the sensors are in tact, the presence of these disturbances can be verified and further characterized.

The two downstream sensing systems that are currently being developed at UCSB are the ultraviolet (UV) absorption monitor and the reflective difference spectroscopy (RDS) sensor. These sensing systems are both optical-based, where a light source is directed at or near the sample and a detector measures the remaining light after either absorption or reflectance occurs. The UV sensor provides real-time information about the pure component flow delivery rates at the reactor and will therefore be used to control both composition and thickness via the injection MFC. Additionally, the UV sensor has been shown to measure the transport transients and delays occurring after a switching event from the injection manifold [8]. This is extremely useful information that can be used to improve the abruptness of device interfaces. The RDS system provides real-time growth rate information [9, 10]. Using the RDS signal information, the growth rate can be regulated by controlling the switching time at the injection manifold.

Still, another reason to apply control to MOCVD growth is to improve the tracking performance to a commanded reference input. The growth of high efficiency vertical-cavity surface-emitting lasers requires the parabolic grading of composition in thin layers [11].

Currently, these gradings are obtained by commanding a mass flow controller to flow the parabolic profile. Although the flow is controlled, the tracking error between the commanded and actual composition is still running in an open loop fashion and can be greatly reduced with compositional feedback control.

2.4 Overview of Control Approach and Status

This project encompasses three types of control loops, which are divided below by the type of sensor. The first loop uses an ultrasonic sensor that is located upstream in the process, at the gas delivery system. The second loop uses an ultraviolet concentration monitor, located downstream in the process, and measures the reactant concentrations just before the susceptor. The third loop uses a reflectance difference spectroscopy sensor, which measures the growth rate of the sample. In future work, one or more of these loops may be combined to obtain an optimal coupled system, but at this stage, the three separate loops are being investigated.

At UCSB, there are two MOCVD machines: one used for the AlGaInP material system and one used for InGaN material system. The AlGaInP MOCVD machine also has nitride capabilities because it is of interest to investigate these material systems with nitrogen. This project encompasses the implementation of all three loops on each machine. The AlGaInP material system has been studied longer and is better characterized in the literature, as compared to the younger InGaN material system. For this reason, the three control loops will be first implemented on the AlGaInP system, then on the InGaN system. Most of the equipment was purchased in duplicate, in order to facilitate the control systems on both MOCVD machines. However, several components were not duplicated in order to allow for testing and improved sensor design.

The status at present is as follows:

- Ultrasonic Sensor for AlGaInP:
  The ultrasonic sensor control has been successfully implemented. However the ultraviolet sensor control loop will actuate the injection MFC. Consequently, the ultrasonic control system was redesigned using a different actuator and must be tested.

- UV sensor for AlGaInP:
  All the components are purchased and the sensing system has undergone successful preliminary tests. Current efforts include reducing the signal-to-noise ratio and optimizing the geometry of the sensor lay-out.

- RDS sensor for AlGaInP:
  All components are purchased. Initial tests of individual components have been performed, for example, remotely driving the monochromator with the motor and

testing the light source and detectors. The next step is to configure the entire system and obtain growth rate signal.

- Ultrasonic Sensor for InGaN:
  Three ultrasonic sensors (one Epison and two Minisons) have been purchased and installed in this system. A closed loop control option has been purchased by the MOCVD manufacturer for the Epison (TMI source). The next step is to compare the differences between the control system we developed and the control system the manufacturer developed.

- UV Sensor for InGaN
  Most of the components have been purchased. This system will be optimized based on the results of the AlGaInP system.

- RDS Sensor for InGaN
  Most of the components have been purchased. This system will be optimized based on the results of the AlGaInP system.

2.5 Applications of Feedback Control

Upstream Ultrasonic Sensor Control

To start, we have developed a mathematical model of the MOCVD process based on first principles and input/output data [1, 12]. From this model, we designed a control system that uses an upstream concentration measurement to control the mass flow rate of one gas. The goal of this controller was to reject the bubbler disturbances that perturb the pure component flow. Initially, we built and tested an analog version of this controller. Then we implemented the controller on the MOCVD system and grew some device-like samples. By comparing the X-ray diffraction results of the samples grown with my control system to the samples grown under normal operation, it was evident that the control system improved both composition and thickness reproducibility [1, 2].

Encouraged by the success of this analog implementation, we developed a corresponding digital control implementation. In general, a digital control system is preferred for control research because the control structure can be modified quickly and easily. In addition to control, the digital system is also used for data acquisition. In recent tests, we have recorded 6 channels of information. With the newly purchased equipment, we will be able to record over 30 signals.

The control system we implemented measured the concentration from the ultrasonic sensor (see Figure 1) and controlled the flow rate at the injection MFC. This was a "feedforward" control structure. Due to its location in the process, the injection MFC is chosen to be the best actuator for the UV absorption loop, which is described in the next section. Consequently, a new control system was configured for the ultrasonic

concentration sensor and is illustrated in Figure 2. The control loop now consists of measuring the concentration and controlling a combination of the carrier and dilution MFCs. Because this is a "feedback" control structure, additional modeling and analyses are required to design the controller. Current control theory efforts involve modeling the nonlinear bubbler dynamics labeled in Figure 2. The performance goals of this loop are to regulate the desired concentration and to reject the previously identified bubbler disturbances. The flow sent downstream will then have a more stable concentration content and will ease the disturbance rejection action in the UV and RDS loops.

The remaining steps in this development include the following:

- Complete the plant modeling effort and feedback controller design
- Implement the control system, closing the loop shown in Figure 2.
- Perform input/output experiments on the closed loop system to further identify the MOCVD process dynamics and disturbances.
- Enhance the current plant model and optimize the controller design.
- Evaluate the control system by growing test structures and performing post-growth material examinations such as X-ray diffraction and photoluminescence to independently verify the composition and thickness control performance.
- Analyze both real-time and post-growth data to improve the control loop.

Downstream Ultraviolet Absorption Sensor Control

The next step in this work is to use an ultraviolet (UV) absorption sensor located at the growth chamber for feedback in a pure component flow control scheme. As shown in the previous section, this will improve both the composition and thickness accuracy and reproducibility. Because this measurement is located just before the growth occurs, it provides better *in situ* information than the upstream ultrasonic concentration signal. A schematic of the UV sensing system is shown in Figure 3. Although the sensor development is not complete, this figure displays the general configuration of the components. The sensor physics is based on Beer's Law where the amount of absorbed light is proportional to the reactant concentration (or partial pressure). The goal in designing this system was to obtain the best signal-to-noise ratio. Hence, the components were purchased with this in mind. As shown in Figure 3, the UV light source is generated using a 30 Watt deuterium lamp. The light is then chopped at a reference frequency, focused and filtered. The filter has a center frequency of 200 nm and a bandwidth of 20nm. It is used to attenuate the visible light. The light is passed through the reaction chamber and hence through the gas mixture of the reactant and hydrogen. Here is where the desired absorption occurs. The remaining scattered light is then refocused

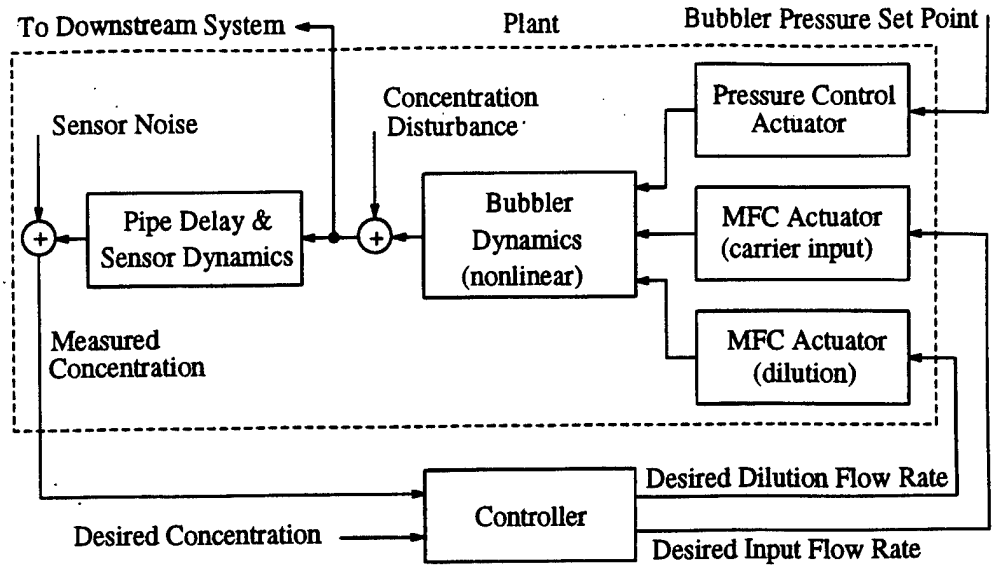

Figure 2: The upstream feedback control loop. The feedback sensor is the ultrasonic concentration monitor. The control actuators are teh input and dilustion mass flow controllers. The controller design goals include regulation of the desired concentration and rejection of the bubbler concentration disturbance.

into the monochromator. The monochromator will be set to pass only one wavelength of light and is equipped with UV enhanced gratings. The monochromator must be located directly in front of the photomultiplier tube (PMT) detector in order maximize the dynamic range of the PMT as well as to protect the light sensitive optical components. The detector signal is amplified at the chopped reference frequency via the lock-in amplifier. This amplified signal is sampled with an A/D converter to be used in the digitally implemented control law. The control output is then reconstructed at the same rate with a D/A converter and is sent to adjust the flow rate of the injection MFC.

This monitoring system is being assembled at present. Preliminary tests were performed to assist in the sensing system component selection. Figure 4 is a plot of the absorption spectra for TMG and TBP. Although these data were obtained with a sub-optimal hardware configuration (key components were not purchased at the time of the test), the absorption profiles are in excellent agreement with the literature [8, 13]. Other tests were performed to determine the best way to direct the light to and from the reactor. It was found that fiber optic cables strongly attenuated light in the UV range and therefore could not be used for light alignment. Alternatively, a system of UV-rated mirrors and lenses were tested and chosen to be the best method of light alignment.

Figure 5 illustrates how the UV sensor will be used in the control loop. The sensor will measure concentration at the reaction chamber and will be combined with the flow measurement to control the injection MFC. The control goals include rejecting

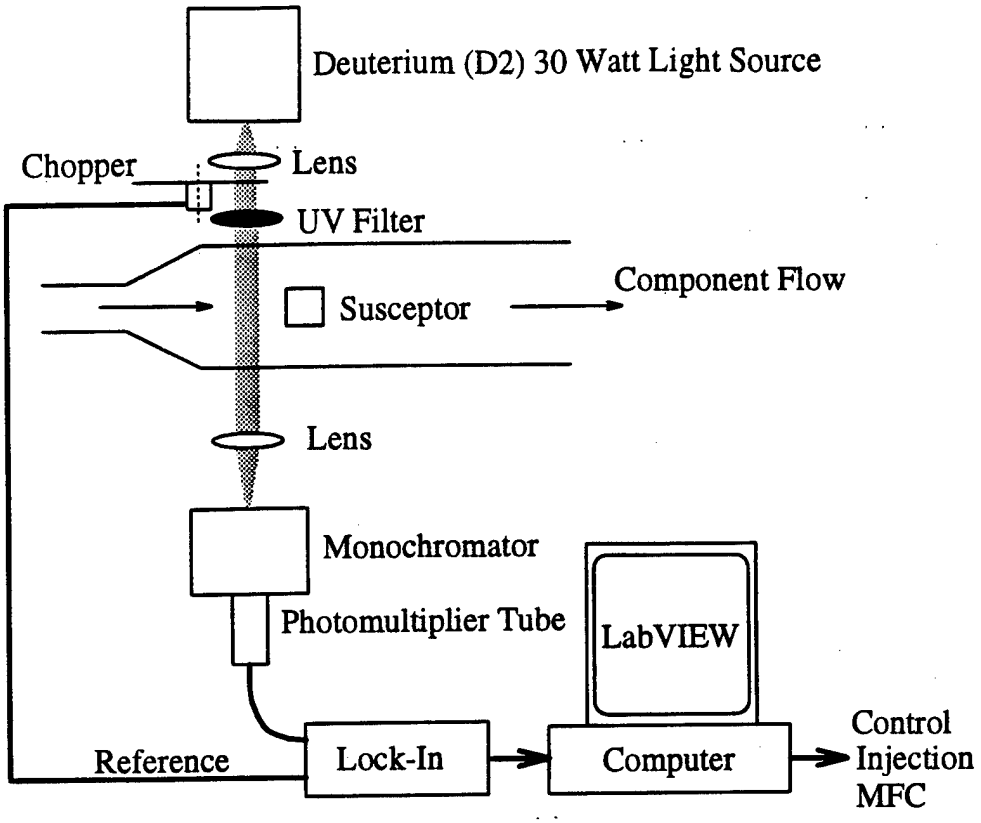

Figure 3: The ultraviolet absorption sensing system. The light is passed through the reaction chamber and hence through the gas mixture of the reactant and hydrogen. Using Beer's law, the reactant partial pressure is determined from the absorption signal. The wavelenghth range of interest is 180nm-230nm.

the pure component flow disturbances and tracking the desired pure component flow trajectory. Recall that the pure component flow is the product of the total flow and the concentration of the reactant in that flow. This relationship is indicated in Figure 5 by the block containing "x". Assuredly, the traditional control objections will be obtained, such as preserving system stability and attenuating high frequency sensor noise.

The remaining steps in this development include the following:

- Obtain the optimal sensor configuration.
- Sensor calibration.
- Perform input/output experiments to identify the MOCVD process dynamics and to characterize the disturbances, which are all represented in Figure 5 in the dashed box entitled "Plant".
- Enhance the current plant model based on the UV input/output data.

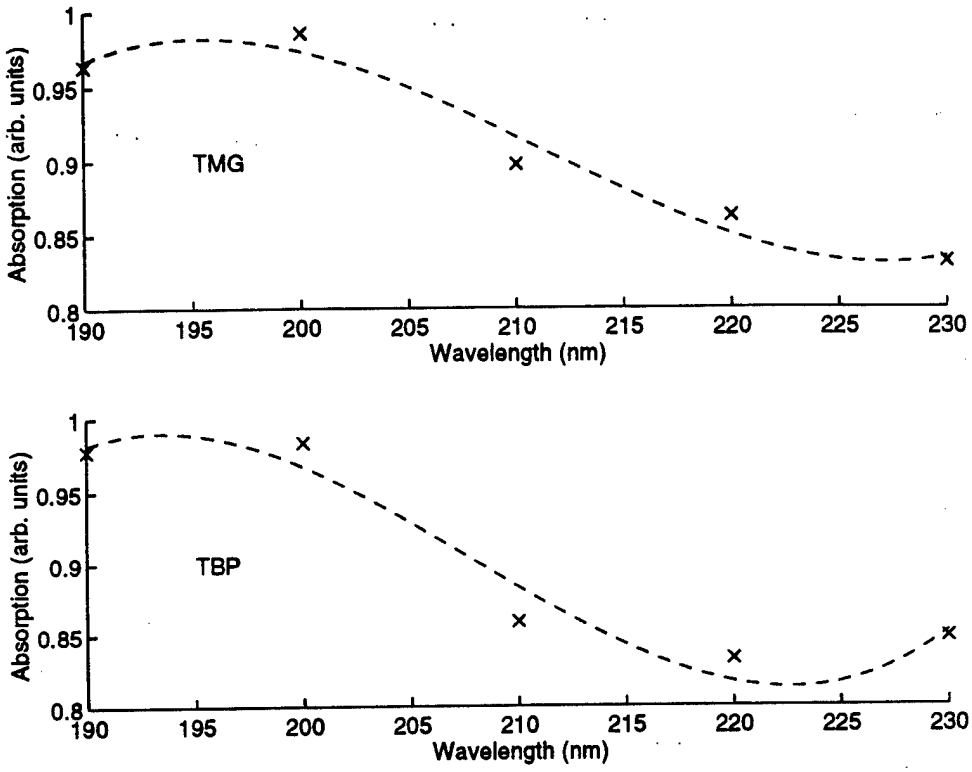

Figure 4: Absorption spectra from a preliminary UV absorption sensing system. These curves were used to verify the absorption peaks. From these test, the wavelength bandwidths of the sensor components were selected. The wavelengths measured include: 190, 200, 210, 200, and 230 nm.

- Design and implement a control system, closing the loop shown in Figure 5.
- Evaluate the control system by growing test structures and performing post-growth material examinations such as X-ray diffraction and photoluminescence to independently verify the composition and thickness control performance.
- Analyze both real-time and post-growth data to optimize the control loop.

This downstream monitoring system was pursued first, over the RDS system, because it is deemed to be optically simplier. Furthermore, the UV loop is similar to the successfully implemented upstream ultrasonic loop because the control goal is to regulate the pure component flow. Since the upstream loop growth results were so promising, similar results are expected here. Finally, the UV monitoring system provides a means to improve the abruptness of device interfaces by measuring the transport transients and delay. For these reasons, the UV sensor will be the first downstream monitor to be implemented.

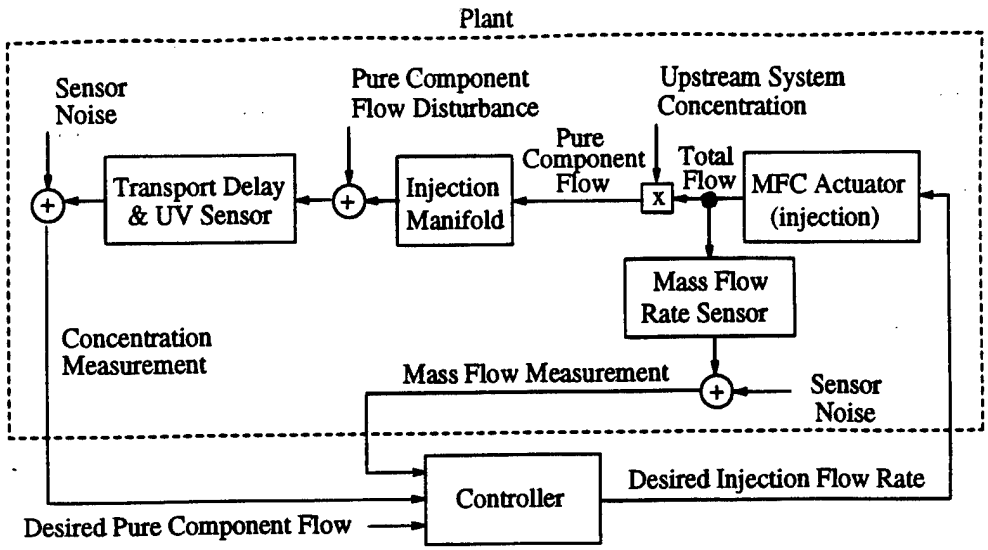

Figure 5: The downsteam closed loop system using the UV sensor for feedback. The control inputs include the desired pure component flow, the measured concentration from the UV sensor, and the measured flow rate at the injection MFC. The control goals include pure component flow tracking in the presence of disturbances.

Downstream Reflective-Difference Spectroscopy Sensor Control

A third control system, based on reflective difference spectroscopy (RDS) information, is being investigated in order to control growth rate (thickness), as opposed to composition. As shown in Figure 6, a polarized light source is reflected from the growing surface and the relative reflectance difference of the light along the two principal axes of the reconstructed surface is measured. This sensor will provide real-time monitoring of the surface reconstruction and monolayer coverage of the growths. Currently, all the RDS components have been purchased. Tests on the individual components have been performed. The next step is to fabricate the entire sensor system.

The closed loop control system using the RDS sensor is illustrated in Figure 7. As shown, the control inputs are the desired and measured growth rates. The control output is a switch command to the injection manifold. The goal here is to use the RDS growth rate information to obtain the desired thickness by regulating the desired growth rate in the presence of disturbances. Preliminary work on the growth model (in Figure 7) can be found in [12]. This work is based on the MOCVD growth models developed by [14].

The remaining steps in this development include the following:

- Configure components and obtain a growth rate signal.
- Characterize the RDS sensor dynamics, the growth system dynamics, and identify

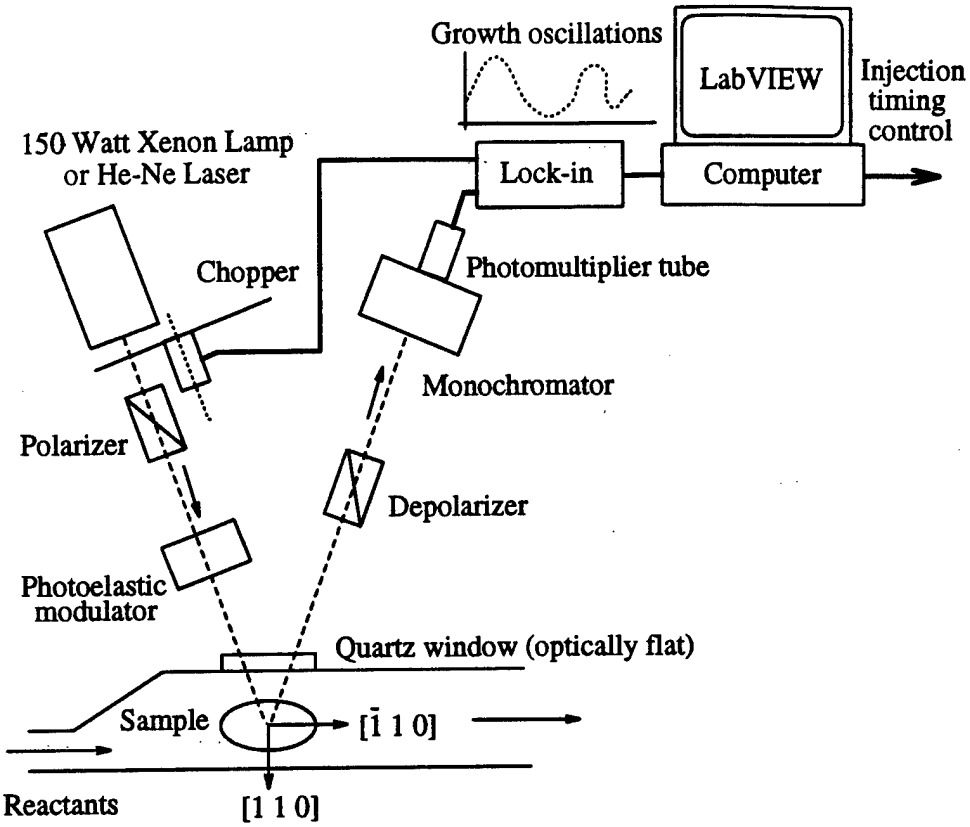

Figure 6: The reflective-difference spectroscopy sensing system used to control growth rate (thickness). A polarized light source is reflected from the growing surface and the relative reflectance difference of the light along the two principal axes of the reconstructed surface is measured. This sensor will provide real-time monitoring of the surface reconstruction and monolayer coverage of the growths.

the disturbances that perturb thickness.

- Improve the existing plant model (components shown in Figure 7) and design a controller to obtain precise layer thickness.
- Implement the controller and evaluate with post-growth tests.
- Improve controller design based on the real-time data and post-growth evaluations.

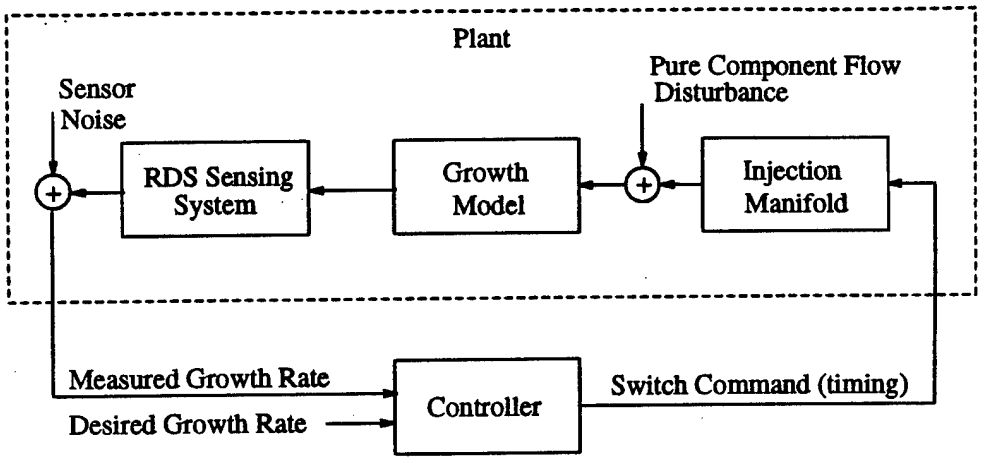

Figure 7: The reflective-difference spectroscopy control loop. The control input is the measured growth rate from the RDS sensor and the control output is the time to switch the reactants at the injection manifold. The control goal is to track a growth rate command in the presence of pure component flow disturbances.

3 Equipment

This section provides details on the equipment purchased under this grant..

3.1 Budget

AlGaInP control hardware (new N capability)	Table for optics and cart for computer (Global Industrial Equipment)	1,000
	Analog/Digital boards (2 @ $895) National Instruments: AT-MIO-16-9	1,790
	Digital/Analog board National Instruments: AT-AO-10	1,170
	Digital Signal Processing Board National Instruments: DSP2200 (256K memory)	2,515
	Connection hardware	600
AlGaInP RDS system	Optical reaction chamber heater (Thomas Swan Ltd.)	9,400
	Computer for data analysis	3,500
	HeNe Laser (Oriel)	400
	Misc. optical components	2,000
AlGaInP UV system	Photodetectors (various vendors)	800
	Misc. optical components	2,000
InGaN UV system	Light source (Oriel)	5,000
	Monochromator (Oriel)	3,100
	Monochromator interface (Oriel)	1,300
	Lock-in amplifier (EG&G/PARC)	3,600
	Photodetectors (various vendors)	800
	Light beam chopper (Oriel)	1,100
	Misc. optical components	2,000
InGaN gas concentration system	Epison II gas composition analyzer (Thomas Swan Ltd.)	14,500
	Epison II closed loop option	750
	Epison II RS232 communications option	225
	Minisons (× 2)	4,800
InGaN control hardware	Control & acquisition computer Pentium (100MHz)	2,500
	Analog/Digital boards (2 @ $895) National Instruments: AT-MIO-16-9	1,790
	Digital/Analog board National Instruments: AT-AO-10	1,170
	Digital Signal Processing Board National Instruments: DSP2200 (256K memory)	2,515
	Connection hardware	600
	GPIB board National Instruments: AT-GPIB/TNT	500
Total:		$71,425

3.2 Description of Acquired Hardware

AlGaInP Control Hardware

1. Work Bench, Power Riser, 30x48 Industrial Cart, Drawer with Lock, Four Outlet Electrical Strip
   Global Equipment Company
   919.75 (88.00)
   The work bench is in the MOCVD clean room across from the MOCVD reactor and is used to hold one computer for control, one computer and printer for data analysis, and the majority of the optical equipment. The industrial cart is used to transport the control computer and various optical equipment to and from the clean room. It is more convenient to do most preparation would in a lab other than the clean room.

2. AT-MIO-16XE-50 + NI-DAQ (Quantity 2)
   National Instruments
   1,791.00
   These two multifunction boards together have 32 analog inputs and 4 analog outputs. The boards are installed in one computer and support the digital implementation of a controller system for the AlGaInP MOCVD system.

3. AT-AO-10
   National Instruments
   1,165.50
   This analog output board has 10 output channels and is used in the digital control implementation of the AlGaInP MOCVD system.

4. AT-DSP2200
   National Instruments
   2,515.50
   This is a 16-bit analog input and 16-bit analog output DSP accelerator board (256 Kword) and supports the AlGaInP digital control implementation.

5. (1 m) 68 to 50 Pin Shielded Cable Assembly (Quantity 2)
   National Instruments
   225.00
   Connection hardware to control boards.

6. (1 m) 50 Pin Ribbon Cable
   National Instruments
   27.00
   Connection hardware to control boards.

7. Surge Protectors (Quantity 2)
   Newark
   36.44

Used to protect the control computer and the data acquisition computer in the clean room.

8. 15 Volts Power Supply (Quantity 2)
   Newark
   31.94
   Used to power the op-amps in the analog anti-aliasing filters, located before the analog-to-digital converters.

9. Isolated BNC Bulkhead Connectors (Quantity 4)
   Newark
   42.80
   These BNC connectors are installed in the back panel of the AlGaInP reactor. They are used to bring signals to and from the reactor deck while preserving the reactor deck seal. As an example, both the photomultiplier tube and the chopper are located on the deck. These instrument signals are sent, via the bulk head connectors, to the lock-in amplifier, which is located on the work bench.

10. (6 Ind. Pair) Shielded Cable
    Newark
    260.26
    The cable is used to interface between the control computer and the MOCVD sensors and actuators.

11. (13in x 17in x 3.5in) Rack
    Newark
    141.52
    This rack fits into the AlGaInP 19in rack and houses anti-aliasing filters, the Epison analog controller and several connector blocks. It is located near the MOCVD sensor and actuator connections.

AlGaInP RDS System

1. Optical Reaction Chamber Heater
   Thomas Swam Ltd.
   9,000.00
   The reaction chamber had to be modified, in order to perform reflective-difference spectroscopy on the growing sample. The modifications included a new reactor and heater. This purchase is the heater contribution, and the new reactor came from another funding source.

2. Power MAC 7500/100, Apple 15in Display, Apple Design Keyboard, MicroPrint Ethertalk
   Machintosh (supplier: UCSB Bookstore)
   2860.04

This computer is housed in the clean room and is used extensively during experiments to analyze data. The convenient location for data analysis expedites progress. In addition, during the slow time of an experiment, for example in growing a two hour layer, the grower can not leave the clean room. During these times, further analysis and writing is performed in the clean room on this computer.

3. LaserWrite Select 360, MAC printer cable (10 ft)
   Machintosh (supplier: UCSB Bookstore)
   1056.88
   This laser printer is housed in the clean room.

4. Red Self-Contained Helium Neon Laser
   Melles Griot
   234.74
   The helium neon laser is used for alignment of the optical components, such as mirrors, lenses, polarizers, and the monochromator. In addition, the laser can be used as the source light in the RDS system.

5. Plate
   Oriel
   127.00
   Used to support optics.

6. (6 in) Rod and Rod Holder (Quantity 2 each)
   Oriel
   112.00
   Used to align optics.

7. Carrier
   Oriel
   84.00
   Used to adjust optics.

AlGaInP UV System

1. Photomultiplier Tube with housing and amplifier
   Hamamatsu Corporation
   1055.27
   This photomultiplier tube can measure both UV and visible light. It will be used in both AlGaInP and InGaN UV experiments. If appropriate, then another PMT will be purchased.

2. 12 Volt Power Supply
   Newark
   14.45
   The 12 volt supply is used to power the photomultiplier tube.

3. Tube Holder
   Oriel
   201.00
   The tube holder will clamp around the PMT housing, enabling alignment and support with the monochromator.

4. (40mm, 80mm, 150mm, 300mm) Mounting Posts (Quantity 1 each)
   Melles Griot
   56.00
   Used to align optics.

5. Post holder (Quantity 2)
   Melles Griot
   44.00
   Used to align optics.

6. Complete Simple Beam Steerer
   Melles Griot
   315.01
   This simple beam steerer is used to change the direction and height of the light from the lamp.

7. X-Y Movable Holes
   Oriel
   97.00
   This interface plate is used to support and adjust optics.

8. Large Table Base
   Oriel
   103.54
   This base plate is used to support optics.

InGaN UV System

1. No Ozone D2 Lamp and socket adapter
   Oriel
   440.00
   The D2 lamp is an excellent source of ultraviolet light and will be used as the light source in all UV absorption experiments. With the socket adapter, this lamp will fit into a previously purchased lamp housing.

2. D2 Power Supply
   Oriel
   1589.00
   This power supply is used to drive the D2 lamp.

3. Monochromator Housing
   Oriel
   1397.33
   The monochromator will be located just before the photomultiplier tube and is used to obtain a single wavelength of light. The photomultiplier tube will be damaged if exposed to high energy levels of light. For this UV application, the light wavelength range of interest is between 180-230 nm.

4. UV Monochromator Gratings (Quantity 2)
   Oriel
   492.00
   These monochromator gratings minimize UV attenuation and are installed in the monochromator when selecting a single wavelength in the UV range.

5. Monochromator Variable Slit (Quantity 2)
   Oriel
   964.00
   The variable slits are located at the inlet and outlet of the monochromator and allow for light beam adjustment.

6. Monochromator Stepper Motor Drive
   Oriel
   499.00
   The monochromator stepper motor enables the adjustment of monochromator wavelength from a computer driver. This is extremely useful during growth because the monochromator may be located on the reactor deck, which is sealed and hence unreachable during an experiment. Additionally, for some UV experiments the measurements will require the computer driver to quickly toggle between several wavelengths.

7. Monochromator Stepper Motor Drive Controller
   Oriel
   1306.00
   The controller is used to drive the monochromator stepper motor as described above.

8. 5209 Single-Phase Lock-In Amplifier
   EG&G Instruments
   4085.44
   The lock-in amplifier is the key component in obtaining a good signal-to-noise ratio of the UV absorption signal. The UV light source is chopped at a frequency that the lock-in amplifier detects. Consequently, the chopped light is the only component of all light detected by the PMT tube that is amplified by the the lock-in.

9. Open Chopper
   Oriel

1091.00
The open chopper is used to chop the light beam at a desired frequency thereby providing a modulated light signal for the lock-in amplifier to detect.

10. 40 Apt. Chopper Wheel
    Oriel
    70.00
    This chopper wheel allows for a maximum chop rate of 4000 Hz.

11. UV Range Bi-Convex Lens Set
    Oriel
    708.00
    These lenses have symmetric surfaces and are used to focus the UV light into the monochromator. This set contains five lenses, each for a different focal length.

12. UV Range Convex Lens Set
    Oriel
    555.00
    These lenses are used to collimate the diverging light from the D2 lamp. This set contains five lenses, each for a different focal length.

13. Optical Holders (Quantity 3)
    Oriel
    192.00
    The optical holders support the lenses described previously.

14. UV Gloves
    Oriel
    27.00
    The UV gloves protect the hands from harmful UV rays while adjusting and aligning equipment with the lamp on.

15. UV Filter
    Oriel
    475.00
    The UV filter has a center frequency of 200 nm with a bandwidth of 20 nm. The filter is used to attenuate the visible light from the D2 lamp.

16. UV Filter Holder
    Oriel
    70.00
    Supports the UV filter.

17. Lab Jack
    Melles Griot
    845.70
    The lab jack supports the D2 lamp and is used to adjust the light source to the height of the reactor.

18. (1 in thick) Plate
    Melles Griot
    175.00
    This plate will be mounted on the lab jack to support optical components that are aligned with the D2 lamp.

19. UV Coated Mirrors
    Melles Griot
    144.58
    The mirrors will be used to direct the UV light beam.

20. Gimbal Mirror Mount (Quantity 2)
    Melles Griot
    762.00
    The gimbal mirror mounts are used to align the UV mirrors. These mounts are compatible with a previously Melles Griot purchased beam steerer.

InGaN Gas Concentration System

1. Epison II Gas Composition Analyzer
   Thomas Swan Ltd.
   14,500.00
   The Epison II is an ultrasonic concentration sensor and is used in the real-time control of growth. Specifically, this sensor is used to monitor the concentration of TMI (trimethlyindium). TMI is the only solid precursor, the others are liquids, and hence has been shown to have the greatest concentration fluctuations, as the solid precursor depletes.

2. Epison II Closed Loop Option
   Thomas Swan Ltd.
   750.00
   The closed loop option allows the grower to use the Epison concentration monitor in a closed loop fashion, where the sensed concentration information is used to adjust the input carrier flow rate, in order to regulate the pure component flow.

3. Epison II RS232 communications option
   Thomas Swan Ltd.
   225.00
   The RS232 connection provides a means for communicating with the remote computer system at the Epison. These signals are of interest because they will be overriding the control commands from the main growth computer system.

4. Minisons (Quantity 2)
   Thomas Swan Ltd.
   4,800.00

The Minison is a less expensive and less accurate measurement of the concentration of a precursor. For the InGaN system, these two concentration sensors are located on the TMG (trimethlygallium) and TMAl (trimethlyaluminum) lines, respectively.

InGaN Control Hardware

1. Pentium 100 MHz, 15 in Monitor
   Inteva (supplier - Insight Direct Inc.)
   2158.00 (252.44)
   This control computer supports the InGaN digital control implementation.

2. 3COM PCI Combocard
   3Com (supplier - Insight Direct Inc.)
   159.00
   This ethernet link expedites the transfer of large data files from the clean room computer to the Identification and Control Laboratory computing facilities.

3. Tapebackup
   Backpack (supplier - Insight Direct Inc.)
   179.00
   The tape back-up is used to store data. Since there are over 40 signals available per run, the data storage is quite extensive.

4. AT-MIO-16XE-50 + NI-DAQ (Quantity 2)
   National Instruments
   1,862.25
   These two multifunction boards have together 32 analog inputs and 4 analog outputs. The boards are installed in one computer and support the digital implementation of a controller system for the InGaN MOCVD system.

5. AT-AO-10
   National Instruments
   1,165.50
   This analog output board has 10 output channels and is used in the digital control implementation of the InGaN MOCVD system.

6. AT-DSP2200
   National Instruments
   2,515.50
   This is a 16-bit analog input and 16-bit analog output DSP accelerator board (256 Kword) and supports the InGaN digital control implementation.

7. Connector Block (Quantity 3)
   National Instruments
   297.00
   Connection hardware to control boards.

8. (1 m) 68 to 50 Pin Shielded Cable Assembly (Quantity 2)
   National Instruments
   225.00
   Connection hardware to control boards.

9. (2 m) 50 Pin Ribbon Cable
   National Instruments
   38.00
   Connection hardware to control boards.

10. RTSI Bus Cable
    National Instruments
    36.00
    Connects all National Instruments boards together for faster control implementation.

11. External GPIB Controller for PC Parallel Port
    National Instruments
    648.00
    The GPIB board is used to control equipment that does not need to change in real-time, but is located on the reactor deck and thus required a computer driver rather than manual control. Typical instruments include the monochromator wavelength, the chopper frequency, and the lock-in amplifier settings.

12. (2 m) GPIB cable
    National Instruments
    72.00
    Connects GPIB controller to PC and experiment.

13. LabVIEW Upgrade
    National Instruments
    191.75
    Controller software coding environment for the National Instruments boards.

14. Surge Protectors (Quantity 1)
    Newark
    18.22
    Used to protect the control computer in the clean room.

4 Summary and Conclusions

Pure component flow control has been shown to improve both the composition and thickness properties of the device growth by using an upstream ultrasonic concentration signal feedback. Both [1] and [2] describe the success of this preliminary pure component flow control system, where the former is addressing a control theory reader and the latter, a crystal growth reader. In this control scheme, the controller objectives were nominal pure component flow regulation and disturbance rejection, remembering that the pure component flow is the product of component concentration and total flow. The controller input was the concentration monitor and the controller output dynamically adjusted the injection MFC set point (both sensor and actuator are shown in Figure 1).

In order to evaluate the effectiveness of the controller, two alloy structures were grown using the same growth recipe. The first structure was grown under open loop conditions and the second under closed loop conditions. The structure grown consisted of alternating layers of InP (indium phosphide) and GaInAs (gallium indium arsenide) , or more specifically, a 5-period $Ga_{0.47}In_{0.53}As$/InP (3000 Å/200 Å) superlattice. Further details of these test growths are described in [2]. A superlattice structure was chosen for several reasons. First, the multilayers investigate composition at defined stages of growth. Second, the superlattice nature acts as a probe to examine both the thickness and composition reproducibility from layer to layer [3]. After the growths, both the open loop and closed loop sample composition and thickness were investigated using X-ray diffraction techniques. As shown in [2], the X-ray results strongly indicated that the closed loop system obtained the target solid composition and thickness in the GaInAs layers far better than the open loop system.

The details of the controller implementation are discussed in [5]. The preliminary controller structure consists of a low-pass filter and static inversion of the concentration signal. The inversion is simply a division of the optimal pure component flow rate (PCF_{opt}), as required for the proper growth, by the concentration signal (C_{meas}). The controller output, therefore, is the injection mass flow rate set point (F_{set}) that satisfies, $PCF_{opt} = C_{meas} \times F_{set}$.

Further pure component flow control, with the UV feedback, will significantly aid the transition of MOCVD techniques from the laboratory to commercial development. Implementation of the RDS based control scheme will lead to precision control of scale in the growth direction, ultimately improving the more advanced commercial applications. Both of these applications require the modeling of the downstream gas delivery dynamics and the actual growth. A preliminary growth model is discussed in [12].

Devices which could immediately benefit from both UV and RDS feedback include LEDs, high electron mobility transistors, resonant tunneling devices, and quantum well laser diodes. Of these devices, the blue light sources are of great interest because the whole visible spectrum can be realized with AlGaInP and the nitrides. This brings

the prospect of an extremely low power consumption white light source using MOCVD technology. The control processing improvements will also further the capabilities in high speed computing and telecommunications.

Closed-loop control also has benefits for MOCVD semiconductor manufacturing processes by providing good reproducibility and thereby allowing for additional flexibility. Production lines may be stopped and the restarted as the market demands vary, because the control systems will compensated for any plant changes that occurred during the switch-over. Both pre-calibration and bubbler warm-up procedures can be significantly reduced or eliminate in a closed-loop system. This leads to large savings in processing time, labor, and source materials. It may also be possible to compensate for some level of MOCVD system component degradation which will allow yields to remain high.

References

[1] M. S. Gaffney, R. S. Smith, A. L. Holmes, Jr., C. M. Reaves, and S. P. DenBaars, "Improved composition and thickness control of III-V epitaxy in a metalorganic chemical vapor deposition process," vol. 3, pp. 2490–95, 34th IEEE CDC, Dec. 1995.

[2] M. S. Gaffney, C. M. Reaves, R. S. Smith, A. L. Holmes, Jr., and S. P. DenBaars, "Control of III-V epitaxy in a metalorganic chemical vapor deposition process: Impact of source flow control on composition and thickness." In press: Journal of Crystal Growth, Dec. 1995.

[3] V. Swaminathan and A. T. Macrander, *Material Aspects of GaAs and InP Based Structures.* Prentice Hall, 1991.

[4] EPISON, Manufactured under licence from Northern Telecom Europe Limited by Thomas Swan and Co. Ltd., Semiconductor Division, Unit 1C, Button End, Harston, Cambridge, CB2 5NX, UK.

[5] M. Gaffney, C. M. Reaves, A. L. Holmes, Jr., R. Smith, and S. P. DenBaars, "Real-time composition and thickness control techniques in a metalorganic chemical vapor deposition process," in *Symposium on Diagnostic Techniques for Semiconductor Materials Processing* (S. W. Pang, ed.), vol. 406, Mater. Res. Soc., 1995.

[6] F. Agahi, C. R. Lutz Jr., and K. M. Lau, "Improvement of gas-switching abruptness for atmospheric pressure organometallic vapor phase epitaxy," *J. Crystal Growth*, vol. 139, pp. 344–50, May 1994.

[7] W. L. Holstein, "Performance of gas saturators in the presence of exit stream temperature gradients and implications for chemical vapor deposition saturator design," *Chemical Engineering Science*, vol. 49, no. 13, p. 2097, 1994.

[8] G. A. Hebner, K. P. Killeen, and R. M. Biefeld, "In situ measurement of the metalorganic and hydride partial pressures in a MOCVD reactor using ultraviolet absorption spectroscopy," *J. Crystal Growth*, vol. 98, pp. 293–301, 1989.

[9] D. E. Aspnes, J. P. Harbison, and L. T. Florez, "Application of reflectance difference spectroscopy to molecular-beam epitaxy growth of GaAs and AlAs," *J. Vac. Sci. Technol. A.*, vol. 6, p. 1327, 1988.

[10] L. Lastras-Martinez, A. Lastras-Martinez, and R. Balderas-Navarro, "A spectrometer for the measurement of reflectance-difference spectra," *Rev. Sci. Instrum.*, vol. 64, pp. 2147–2152, August 1993.

[11] M. G. Peters, D. B. Young, F. H. Peters, J. W. Scott, *et al.*, "17.3% peak wall plug efficiency vertical-cavity surface-emitting lasers using lower barrier mirrors," *IEEE Photonics Technology Letters*, vol. 6, pp. 31–3, Jan 1994.

[12] M. S. Gaffney, C. M. Reaves, R. S. Smith, A. L. Holmes, Jr., and S. P. DenBaars, "Modeling and control of a metalorganic chemical vapor deposition process for III-V compound semiconductor epitaxy." To be presented at the 13th World Congress IFAC, July 1996.

[13] H. Ito, S. Watanabe, and H. Yajama, "Ultraviolet absorption spectra of metalorganic molecules diluted in hydrogen gas," *J. Crystal Growth*, vol. 93, pp. 165–169, 1988.

[14] G. Stringfellow, *Organometallic Vapor-Phase Epitaxy: Theory and Practice.* Academic Press, 1989.

A Appendices

A.1 Advanced Degrees

While working towards their Ph.D. degrees, this equipment grant has been extremely useful to the following scientific personnel:

Monique S. Gaffney
Department of Electrical and Computer Engineering

Casper M. Reaves
Department of Materials

Archie L. Holmes, Jr.
Department of Electrical and Computer Engineering

A.2 Publications

This section contains the four publications generated thus far from this project.

M. S. Gaffney, R. S. Smith, A. L. Holmes, Jr., C. M. Reaves, and S. P. DenBaars, "Improved composition and thickness control of III-V epitaxy in a metalorganic chemical vapor deposition process," vol. 3, pp. 2490–95, 34th IEEE CDC, Dec. 1995.

M. S. Gaffney, C. M. Reaves, R. S. Smith, A. L. Holmes, Jr., and S. P. DenBaars, "Control of III-V epitaxy in a metalorganic chemical vapor deposition process: Impact of source flow control on composition and thickness." In press: Journal of Crystal Growth, Dec. 1995.

M. Gaffney, C. M. Reaves, A. L. Holmes, Jr., R. Smith, and S. P. DenBaars, "Real-time composition and thickness control techniques in a metalorganic chemical vapor deposition process," in *Symposium on Diagnostic Techniques for Semiconductor Materials Processing* (S. W. Pang, ed.), vol. 406, Mater. Res. Soc., 1995.

M. S. Gaffney, C. M. Reaves, R. S. Smith, A. L. Holmes, Jr., and S. P. DenBaars, "Modeling and control of a metalorganic chemical vapor deposition process for III-V compound semiconductor epitaxy." To be presented at the 13th World Congress IFAC, July 1996.

M. S. Gaffney, R. S. Smith, A. L. Holmes, Jr., C. M. Reaves, and S. P. DenBaars, "Improved composition and thickness control of III-V epitaxy in a metalorganic chemical vapor deposition process," vol. 3, pp. 2490–95, 34th IEEE CDC, Dec. 1995.

Improved Composition and Thickness Control of III-V Epitaxy in a Metalorganic Chemical Vapor Deposition Process

Monique S. Gaffney*, Roy S. Smith*, Archie L. Holmes, Jr.*,
Casper M. Reaves† and Steven P. DenBaars†

Abstract

Metalorganic chemical vapor deposition (MOCVD) is a promising technology for the fabrication of high speed electronic and opto-electronic devices. Commercial application of this technique is limited by a high degree of process variance. This paper describes work in progress on the development of a closed loop MOCVD facility for GaAs device fabrication. Critical system disturbances, which degrade the growth rate uniformity and reproducibility, and subsequent device performance, are identified. A control system is designed and implemented to regulate the supply of gallium to the reactor. The controller performance is investigated by growing GaInAs/InP superlattices. Post-growth tests clearly illustrate that the compensated samples have better precision in alloy composition and thickness.

1 Introduction

Metalorganic chemical vapor deposition (MOCVD) has become a common method for performing compound semiconductor epitaxy. However, it currently suffers from lack of *in situ* process control which causes a lack of precise reproducibility. Precise control of the compositions and growth rates will allow the construction of a number of high performance III-V semiconductor devices. These include electron mobility transistors [1], resonant tunneling devices [2, p. 278] and quantum-well laser diodes [3]. These devices require precise monolayer level control of the scale in the growth direction.

MOCVD technology has also been used to fabricate high brightness light emitting diodes (LEDs) using AlGaInP based devices [4]. The $(Al_xGa_{1-x})_{0.5}In_{0.5}P$ quaternary alloy is lattice-matched to GaAs and is a direct bandgap semiconductor in the compositions range $0 \leq x \leq 0.7$ (approx.). This corresponds to bandgap energies (emission wavelengths) in the range 1.9eV (650nm) to 2.2eV (560nm) resulting in high-brightness red and yellow LEDs, with efficiencies an order of magnitude greater than conventional devices. Including nitride material systems (as in GaN, $Ga_xIn_{1-x}N$, and $Al_xGa_{1-x}N$ [5]) opens the possibility of developing blue (450nm) and ultraviolet wavelength sources.

There has been a significant increase in interest in the control of semiconductor process within the control community. For example, see the recent work on rapid thermal processing [6, 7, 8], reactive ion etching [9, 10], and plasma deposition [11]. The control issues that arise depend strongly on the characteristics of the process under consideration. Typical issues are: the development of *in situ* sensors, disturbance characterization, and control motivated system modifications. The work presented here addresses these issues for a research scale MOCVD process.

2 MOCVD Technology

In MOCVD growth of III-V semiconductors, a column III alkyl source, such as trimethylgallium (TMGa), is mixed in the vapor phase with an organometallic column V source, such as tertiarybutylarsine (TBAs), and the reactants are simultaneously injected into the growth chamber where they thermally decompose to form single crystal layers. The substrate in the reaction chamber is held at a controlled temperature, typically in the range 500 to 750 °C. In this range the growth rate is determined primarily by the component mass transport, rather than the reaction kinetics. Under these conditions we can make the following assumptions: the incorporation of column III atoms is dependent solely on the amount of column III source vapor introduced into the reactor cell; column III precursor molecules are fully decomposed; and column V source vapor is supplied in excess and does not impact growth rate or alloy composition [12]. Under these assumptions the solid alloy composition and growth rate depend, to first order, on the amount of column III source vapor and the growth rate and alloy composition are linear functions of vapor compositions.

The UCSB MOCVD facility uses a Thomas Swan (U.K.) built reactor, an ultra-fast gas switching manifold and an Epison ultrasonic cell concentration monitor. The column III and the column V organic source materials (which include tertiary-

*Electrical and Computer Eng. Dept. UC Santa Barbara, CA 93106 (gaffney@ruapehu.ece.ucsb.edu)
†Materials Dept. UC Santa Barbara, CA 93106

butylarsine (TBAs), tertiarybutylphosphine (TBP), trimethylgallium (TMGa), trimethylindium (TMIn), and trimethylaluminum (TMAl)) are stored in solid or liquid phase and are kept in a temperature and pressure controlled environment. A hydrogen bubbler system generates the gaseous components. This has significant safety advantages over the more common gaseous sources but introduces additional disturbances due to gas bubbler dynamics.

The separate gases are mixed in an injection manifold, then sent to the growth chamber to thermally decompose onto the substrate. A fast switching manifold prevents dead spaces and the premature component reactions, leading to interfaces with the desired abruptness. Gas molecules in the chamber diffuse through a stagnant layer to the substrate which then decompose on the surface. Products of the decomposition move over the surface until they find available lattice sites where they are incorporated into the lattice [13, p. 135]. The susceptor is under tight temperature control (via IR lamps) to provide uniform film composition and thickness across the substrate. The growth conditions at UCSB include a 500 to 750 °C substrate temperature, atmospheric reactor pressure and 2.8 to 10 Å/s growth rates. Device specific parameters, such as layer thicknesses, and source flow rates, can be found in [14, 15, 16].

3 A Control Problem

We discuss the more important regulation situations in the MOCVD facility, listed in the order of occurrence in the process. A schematic overview of the process for a single source is shown in Figure 1. The source baths are under both temperature and pressure control to provide for a constant evaporation rate from the source chemical. In addition, the source concentration is regulated by three mass flow controllers (MFC1, MFC2, and MFC3). This paper addresses the regulation of pure component flow (PCF) rate, which includes the concentration regulation problem as a subproblem.

From the bubbler system, the reagent gases flow through pipes heated to maintain the reagent gas vapor phase and prevent pipe deposits and clogging. There is a complex system (not shown in Figure 1) involving bypass lines, make-up lines, and a differential pressure controller, to maintain a constant flow out of the bubbler system, and a constant pressure in the reactor. The valve switching associated with this system causes transient flow (and growth) disturbances which can be as short as 0.2 s [14].

The reactant susceptor is under strict temperature control to ensure uniformity of deposition across the wafer. Uniformity in not a severe problem in this reactor as the substrate is only 2 cm^2 in size.

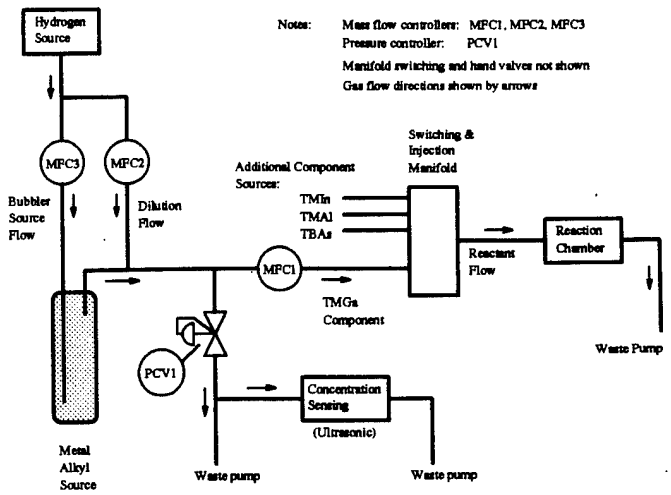

Figure 1: Simplified schematic overview of the MOCVD process for one source (TMGa)

Regulation of the PCF rate was selected as the first control problem to address for the following reasons. The primary performance requirements are precise device composition and thickness. Composition can be controlled (to first order) by the PCF and thickness can be controlled (to first order) by the rate of growth—related to PCF rate and other growth parameters. A simplified explanation of the composition and thickness effects on device performance is as follows. A typical III-V device, for example a quantum-well laser, is made up of different heterolayers of material, starting with the substrate that has a certain lattice constant. Each subsequent layer grown is lattice matched to the substrate lattice constant. If lattice mismatch occurs, the resulting strain can cause a dislocation, leading to severe degradation of the electrical or opto-electrical properties of the device. During a growth, different heterolayers are deposited, each with a toleranced thickness and a toleranced composition. To obtain the required composition for lattice-matching, for example the quaternary alloy $(Al_xGa_{1-x})_{0.5}In_{0.5}P$ is lattice-matched to GaAs, the pure component flow of each column III precursor must be regulated.

In addition, device performance also depends upon the layer thickness. This is particularly true in quantum-well layers, which define the device band gap energy, for devices such as 632.8 nm red LEDs and 1.55 μm quantum-well lasers. In multiple quantum-well lasers, distributed Bragg reflectors and microcavity LED's, variations in layer composition or thickness, will severely compromise device performance [17].

While composition control is primarily a PCF control problem, thickness control is a more difficult growth rate problem. However, the results reported in this work strongly indicate that controlling the

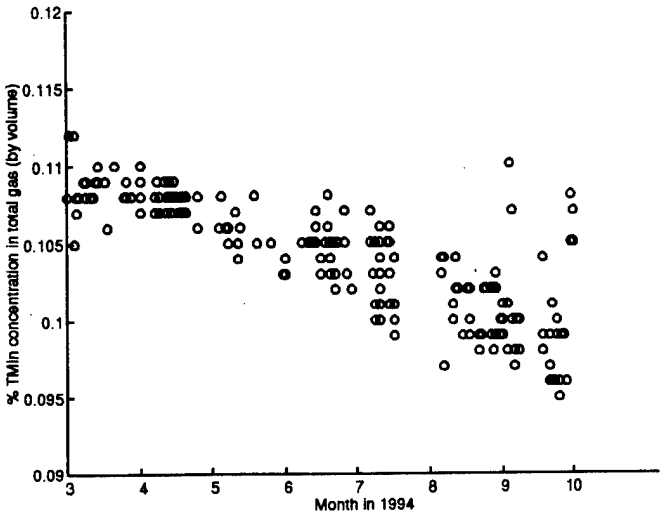

Figure 2: Daily variation of TMIn concentration

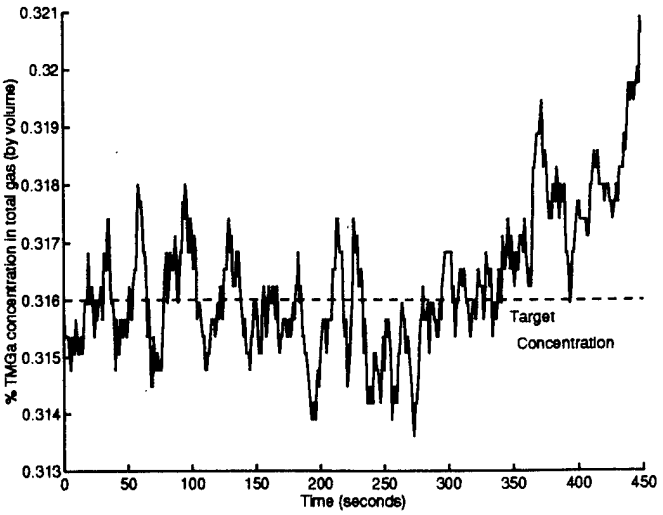

Figure 3: Concentration variation of TMGa during a run

PCF of the column III precursors will, to a large degree, regulate the growth rate as well as the composition. Previous work on feedback control of PCF is reported in [18]. In a materials research environment, obtaining precise composition and thickness takes precedence over obtaining precise uniformity across the wafer. Nevertheless, uniformity is still considered important and is addressed with the susceptor temperature loop previously mentioned and with the reactor design itself.

4 PCF Control Issues

The PCF rate is the product of the precursor concentration and the corresponding mass flow rate into the reactor. This mass flow consists of both the precursor vapor and the carrier gas, and is termed the total flow (for one source line). PCF expresses the amount of gas injected as a volume—partial pressure or the number moles injected are equivalent measures. In a typical facility the PCF rate is adjusted to the desired concentration (according to a device growth recipe) in an open-loop manner by setting the source concentration and mass flow rate independently, before growth. Source concentration fluctuations therefore act as disturbances to the desired PCF.

The PCF regulation system for a single source in the UCSB MOCVD facility is shown in Figure 1. The mass flow controllers MFC3 and MFC2 set the hydrogen entering the bubbler and the hydrogen/component dilution respectively. The pressure controller PCV1 maintains a desired bubbler pressure, allowing for repeatable mixing of the source vapor and the hydrogen carrier. The MFC2, MFC3, and PCV1 set points provide a desired source concentration and are adjusted only rarely.

The mass flow controller MFC1 regulates the mass flow rate into the reactor and is used as the primary control of the PCF. This MFC1 set point is typically adjusted open-loop during the pre-growth set-up procedure to give the desired PCF (measured by using the ultrasonic concentration monitor).

The daily variation of a column III source (TMIn) is illustrated in Figure 2. The concentration decreases approximately 0.01 % in seven months, and increases in variability as the source depletes. Disturbances over this time scale are compensated for by a lengthy pre-growth calibration procedure. Feedback control of PCF will reduce the need for (and/or duration of) such a procedure.

Concentration disturbances are significant during a growth run. Figure 3 illustrates the percent concentration of TMGa flowing in hydrogen during a typical growth run. The target concentration of 0.316 % was preset according to the growth recipe. The deviation from this set point will have a detrimental effect on the growth of the structure between layers, or within a single layer.

The faster disturbances are due to the bubbler dynamics. A slower drift in concentration is also evident—it typically increases, during a run, at a rate of 1×10^{-5} % (by volume)/s. Experiments that distinguish between the bubbler drift disturbances and the Epison sensor noise are reported in [19].

On-line feedback control is required to compensate for disturbances on this time scale. Although a change in concentration of 0.001 % corresponds to approximately 150 ppm (0.015 %) error in the lattice matching and under 1000 ppm is still considered by growers to be lattice matched, the cumulative error in all the sources can cause lattice mismatch and

dislocations to occur.

Closed loop control of the PCF will not only streamline the growth procedure for manufacturing purposes by reducing or eliminating pre-calibration, but will also improve the accuracy of the device composition and the precision of the layer thickness.

5 PCF Based Control

A block diagram of a *single gas* loop model for PCF control is illustrated in Figure 4. The growth recipe specifies the time period for flow based on growth rate estimates. The nominal PCF is corrupted by the concentration and flow disturbances discussed previously.

The controller input is the product of the concentration measurement and the mass flow rate measurement. The Epison monitor measures the speed of sound of the input binary gas mixtures and determines the gas concentrations. The Epison sensor in the UCSB MOCVD reactor was installed for open-loop precalibration of the gases and is located in a bypass line. This has the disadvantages of introducing a measurement delay (approximately 2 s), and allowing the measurement of only a single gas at a time. As a result of this work, the next generation MOCVD reactor, currently under construction, will have in-line concentration sensors for both TMGa and TMIn sources. For system analysis and simulation purposes, the Epison sensor was modeled as a 2 Hz first order lag, cascaded with a 2 s time delay.

The mass flow measurement is taken from the MFC1 local loop, which senses flow rates in the 0 to 100 sccm (standard cubic centimeters per minute) range. Direct measurement of the PCF is not possible—we reconstruct it from concentration and flow measurements—hence the term *observed* PCF. Actuation is accomplished through the set point of MFC1. For analysis purposes, the MFC1 local loop is modeled as a 1 Hz, first order lag.

The controller implementation uses the concentration measurement as an input and the nominal MFC1 flow set point as an output. This is a preliminary strategy that was first investigated for TMIn [18]. Later designs will incorporate the mass flow measurement as an additional controller input. The initial experiments reported below used a static controller. The controller output is a mass flow rate set point, F_{set}, that satisfies, $PCF_{\text{nom}} = C_{\text{meas}} \times F_{\text{set}}$, where PCF_{nom} is the PCF specified by the growth recipe and C_{meas} is the Epison concentration measurement.

6 Experiments and Results

A multilayer structure was designed and grown to evaluate the effectiveness of the feedback control system. After growth, the composition and thickness

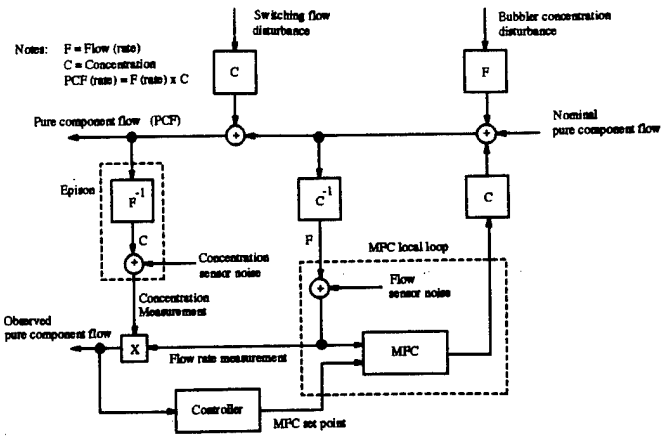

Figure 4: Model diagram for pure component flow control

variations were investigated using X-ray diffraction (XRD) techniques, which are described later. The structure grown (illustrated in Figure 5) consisted of alternating layers of InP and GaInAs, which exhibited the behavior of a 4-period GaInAs/InP (3000 Å/200 Å) superlattice. The nominal layer thicknesses and growth times are shown in the figure. The multilayer feature of the structure allows the investigation of composition at defined stages of growth. The superlattice nature acts as a probe to examine both the thickness and composition reproducibility from layer to layer [13]. The GaInAs layer thickness was chosen to give a sufficiently strong X-ray diffraction signal from each layer, without significantly attenuating the signal from lower layers. The structure was grown under both open loop and closed loop conditions. The controller regulates only the pure component flow of TMGa, so even with closed loop control, disturbances in the other (open-loop) sources can corrupt the composition of the alloy.

The experimental growth begins with the 1000 Å InP buffer layer, which was grown at a faster rate than the subsequent layers. The five GaInAs layers were grown to be nominally 3000 Å thick at a target growth rate of 14 Å/s. The 200 Å InP spacer layers were grown with a nominal growth rate of 2.7 Å/s. The reactor pressure was 760 Torr and the sample temperature was 645 °C. The substrates were epi-ready InP (100), Fe doped, with a 2 degree vicinal misorientation. For these experiments, the desired $Ga_xIn_{1-x}As$ composition is x = 0.47.

For our growth conditions, a TMGa concentration of approximately 0.192 % (by volume) is injected at a flow rate of 90.6 sccm, giving a TMGa pure component flow rate of 0.174 sccm. This is equivalent to a molar flow rate of 7.8×10^{-6} moles per minute and an injected partial pressure of 24.7×10^{-3} Torr. Under these growth conditions, the lattice matching error band is approximately ± 1000 ppm. Exact lattice

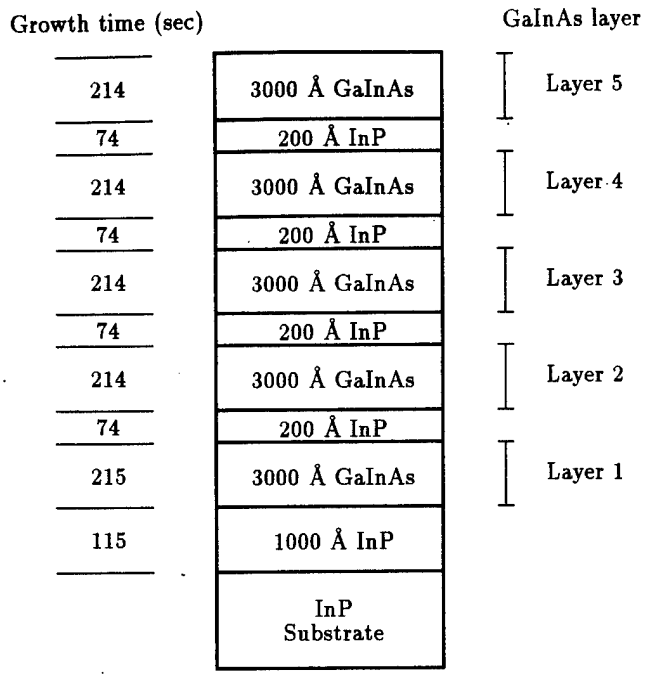

Figure 5: Experimental growth structure

matching is not desired in order to obtain two composition peaks in the X-ray diffraction data. Hence, the growth formula was not tuned to obtain a smaller error band.

Samples were measured with a double-crystal X-ray diffractometer using Cu $K\alpha_1$ radiation and (004) reflection. The XRD technique involves pointing a single wavelength X-ray source at the sample at some incident angle and measuring the diffracted X-ray count. The sample is rocked to vary the angle of incidence and at critical angles of incidence constructive interference (as predicted by Bragg's law) is observed. The plot of X-ray count versus rocking angle is known as a rocking curve.

If the desired structure grown was a ($Ga_xIn_{1-x}As$) layer on an InP substrate, one would expect two peaks in the rocking curve, the first for the InP lattice and the second for the GaInAs lattice. A full-width, half-maximum parameter is used to characterize the quality of the substrate or growth layer crystal lattice. A smaller width implies a more accurate composition.

The relative angle between the substrate and layer peaks can be used to determine the lattice mismatch, which can then be related to the desired composition to verify the alloy molar breakdown.

In multilayered structures (as grown here) higher order constructive interference patterns generated by the lower layers show up as satellite peaks on the rocking curve. In superlattice structures, the presence of satellite peaks is used as a measure of high crystalline quality where both the thickness and composition of the periods are precisely repeated.

Figure 6 shows the rocking curves from both open and closed loop growths of the test structure. The compensated growth contains eight orders of well-defined satellite peaks [19], indicating a significant growth and device quality improvement. The satellite peaks in the closed-loop plot indicate that both the thickness and composition of the GaInAs layers were well regulated. The improved composition control is also evident from the reduced width of the main, closed-loop GaInAs lattice peak (note that it is corrupted by the convolution with satellite peaks).

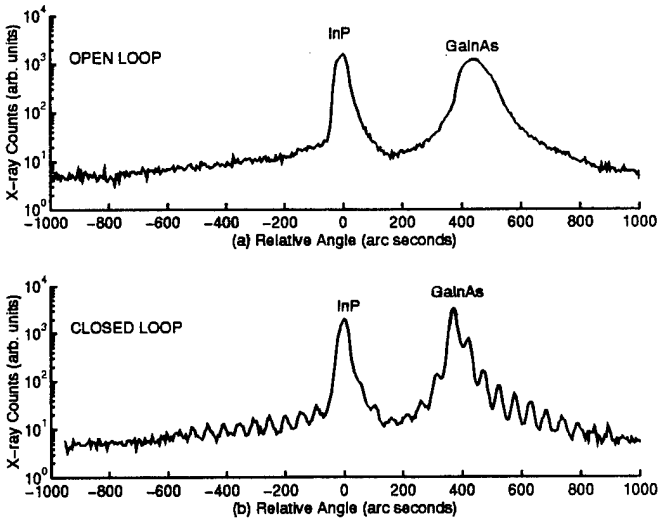

Figure 6: (Log) X-ray diffraction rocking curves for open- and closed-loop growths in normal operation

7 Discussion

The PCF control scheme has been shown to improve both the composition and thickness properties of the device growth by using a concentration signal feedback. We have demonstrated that closed-loop control can significantly improve individual device quality. Closed-loop control also has benefits for MOCVD semiconductor manufacturing processes by allowing for additional flexibility. Both pre-calibration and bubbler warm-up procedures can be significantly reduced or eliminate in a closed-loop system. This leads to large savings in processing time, labor, and source materials. It may also be possible to compensate for some level of MOCVD system component degradation which will allow yields to remain high. An example of this scenario (using a TMGa temperature bath degradation) was illustrated in [19].

We note that the major difficulties in controlling this process do not arise from control design method-

ology issues — a simple static nonlinear controller was effectively used here. The technological issues to be addressed are: control related modeling of the process; model based sensing and sensor characterization; disturbance characterization; control effectiveness quantification in terms of device performance, and control motivated reactor design modifications. Our current, and future, work addresses these issues.

Acknowledgements

The authors would like to thank Jessy Grizzle for useful discussions.

The instrumentation, and a part of the control work was supported by the ARPA Optoelectronic Technology Center (OTC) under contract MDA 972–94–1–0002. The work of C. Reaves was supported by the NSF Science and Technology Center for Quantized Electronic Structures (QUEST) under contract number DMR 91–20007. The work of M. Gaffney and R. Smith was supported in part by NSF under contract ECS–9308917.

References

[1] L. Pfeiffer, K. W. West, H. L. Stormer, and K. W. Baldwin *Appl. Phys. Lett.*, vol. 55, p. 1888, 1989.

[2] H. Heinrich, G. Bauer, and F. Kuchar, *Physics and Technology of Submicron Structures*, vol. 83 of *Springer Series in Solid-State Sciences*. Springer-Verlag, 1988.

[3] J. H. Lee, K. Y. Hseih, Y. L. Hwang, and R. M. Kolbas *Appl. Phys. Lett.*, vol. 56, p. 626, 1990.

[4] Y. Ohba, M. Ishikawa, H. Sugawara, M. Yamamoto, and T. Nakanisi, "High quality InGaAlP epilayers by MOCVD using methyl metalorganics and their application to visible semiconductor lasers," *J. Crystal Growth*, vol. 77, p. 637, 1986.

[5] S. Nakamura, M. Senoh, and T. Mukai, "P-GaN/N-InGaN/N-GaN double heterostructure blue-light-emitting diodes," *Jpn. J. Appl. Phys.*, vol. 32, pp. L8–L11, January 1993.

[6] P. Gyugyi, Y. Cho, G. Franklin, and T. Kailath, "Control of rapid thermal processing: A system theoretic approach," in *Proc. IFAC World Congress*, vol. 7, pp. 93–97, 1993.

[7] J. Stuber, I. Trachtenberg, T. Edgar, J. Elliot, and T. Breedijk, "Model-based control of rapid thermal processes," in *Proc. IEEE Control Decision Conf.*, pp. 79–85, 1994.

[8] A. Emami-Naeini, M. Kabuli, and R. Kosut, "Finite-time tracking with actuator saturation: Application to RTP temperature trajectory following," in *Proc. IEEE Control Decision Conf.*, pp. 73–78, 1994.

[9] M. Elta, J. Freudenberg, M. Giles, J. Grizzle, P. Kabamba, P. Khargonekar, S. Lafortune, S. Meerkov, B. Rashap, D. Teneketzis, and J. F.L. Terry, "Application of control to semiconductor manufacturing reactive ion etching," in *Proc. Amer. Control Conf.*, pp. 2990–2997, 1993.

[10] E. Hamby, P. Kabamba, and S. Meerkov, "A system-theoretic approach to modeling and analysis of deposition rate uniformity in PECVD," in *Proc. IEEE Control Decision Conf.*, pp. 86–90, 1994.

[11] L. Layeillon, A. Dollet, J. Couderc, and B. Despax, "Analysis and modelling of plasma enhanced cvd reactors. Part II: Model improvement and systematic use," *Plasma Sources, Science & Tech.*, vol. 3, pp. 72–79, 1994.

[12] G. B. Stringfellow, *Organometallic Vapor-Phase Epitaxy: Theory and Practice*. Academic Press, 1989.

[13] V. Swaminathan and A. T. Macrander, *Material Aspects of GaAs and InP Based Structures*. Prentice Hall, 1991.

[14] M. Heimbuch, A. Holmes, Jr., C. Reaves, M. Mack, S. DenBarrs, and L. Coldren, "Tertiarybutylarsine and tertiarybutylphosphine for the MOCVD growth of low threshold 1.55 μm $In_xGa_{1-x}As/InP$ quantum-well lasers," *J. Elec. Mat.*, vol. 23, no. 2, pp. 87–91, 1994.

[15] I. Moerman, G. Coudenys, and P. Demeester, "Influence of gas mixing on the lateral uniformity in horizontal MOVPE reactors," *J. Crystal Growth*, vol. 107, pp. 175–180, 1991.

[16] A. Holmes, Jr., M. Heimbuch, and S. DenBaars, "Strained GaInAsP single-quantum-well lasers grown with tertiarybutylarsine and tertiarybutylphosphine," *Appl. Phys. Lett.*, vol. 63, pp. 3417–3419, December 1993.

[17] J. Blondelle, H. D. Neve, P. Demeester, P. V. Daele, R. Baets, and G. Borghs, "Layer thickness and composition control for the fabrication of high efficiency microcavity LED's," in *Sixth European Workshop on Metal-Organic Vapour Phase Epitaxy and Related Growth Techniques*, June 1995.

[18] J. Stagg, J. Christer, E. Thrush, and J. Crawley, "Measurement and control of reagent concentrations in MOCVD reactor using ultrasonics," *J. Crystal Growth*, pp. 98–102, May 1992.

[19] M. S. Gaffney, C. M. Reaves, R. S. Smith, A. L. Holmes, Jr., and S. P. DenBaars, "Control of III-V epitaxy in a metalorganic chemical vapor deposition process: Impact of source flow control on composition and thickness," *J. Crystal Growth*, September 1995. (submitted).

M. S. Gaffney, C. M. Reaves, R. S. Smith, A. L. Holmes, Jr., and S. P. DenBaars, "Control of III-V epitaxy in a metalorganic chemical vapor deposition process: Impact of source flow control on composition and thickness." In press: Journal of Crystal Growth, Dec. 1995.

Control of III-V Epitaxy in a Metalorganic Chemical Vapor Deposition Process: Impact of Source Flow Control on Composition and Thickness

Monique S. Gaffney*, Casper M. Reaves**, Roy S. Smith*,
Archie L. Holmes, Jr.* and Steven P. DenBaars**

* Department of Electrical and Computer Engineering, University of California,
Santa Barbara, CA, 93106 United States

**Department of Materials, University of California,
Santa Barbara, CA, 93106 United States

Revisions submitted to
Journal of Crystal Growth
December 21, 1995

Abstract

A procedure for developing a real-time automated control system for improving epitaxial growth of semiconductors is presented and applied to GaInAs growth by metalorganic chemical vapor deposition. Vapor concentration variations of the gallium source are identified as a primary disturbance. An analog control system that regulates the supply of gallium is designed and implemented. Key issues in the controller synthesis are outlined. The controller performance is investigated by growing GaInAs/InP superlattices. Results of growths performed under normal operating conditions and also under large perturbations are presented. These results include X-ray diffraction from the samples as well as real-time data from the concentration monitor and the flow measurement. High quality superlattices that display up to eight orders of satellite peaks are obtained under closed loop control, demonstrating improved layer to layer reproducibility of thickness and composition.

1 Introduction

1.1 Background

As the requirements for semiconductor materials and devices become more demanding, technologies involved in the processing must improve their ability to create predictable and reproducible structures. To facilitate this, there have been recent efforts in developing sensors and control system methodologies for semiconductor processing. Rapid thermal processing [1, 2], reactive ion etching [3, 4], and plasma deposition [5] are three such processes where a number of parameters have significant effects on the sample quality. The control issues that arise depend strongly on the characteristics of the process under consideration, but typically include issues of disturbance characterization, sensor development, and control-motivated system modification.

Recently, these control issues have been explored for the epitaxial growth of semiconductor layers. Crystal growth technologies, such as metalorganic chemical vapor deposition (MOCVD), require the ability to control composition and layer thickness to high accuracy for device applications such as distributed Bragg reflectors [6], microcavity LED's [7], and high mobility layers [8]. With most growth techniques there are a number of parameters which affect the quality of the semiconductor material; these parameters are difficult, if at all possible, to directly monitor and control. A primary objective of the work herein is to determine the cause of and compensate for disturbances in these parameters. Some parameter disturbances exhibit fast time constants that fall within the duration of a single run.

These disturbances may be of a layer-to-layer nature or may occur within a single layer. Since the time scales in epitaxial growth are often on the order of minutes and seconds, it is prudent to automate a response to these variations. An automatic control system depends on sensors for information. During growth, these monitors typically deal with the sample temperature, layer thickness, state of the sample surface, or vapor concentration. Regardless of the monitoring technology utilized, the next step for epitaxial technology is to further develop these monitoring capabilities and incorporate them into a control system framework [9, 10, 11, 12, 13].

1.2 Control Issues

A schematic overview of the process for a single precursor source is shown in Fig. 1. The sources used in this work, tertiarybutylarsine (TBAs), tertiarybutylphosphine (TBP), trimethylgallium (TMGa), and trimethylindium (TMIn), are each maintained at a constant temperature to provide for a constant evaporation rate from the precursor chemical. In addition, the source concentration is also regulated by three mass flow controllers (MFC's) and a pressure controller (PCV-1). Control of this vapor concentration is essential to obtain precise thicknesses, and solid compositions in the case of an alloy layer. The mass flow controllers (MFC-1) and (MFC-2) set the hydrogen entering the bubbler and the hydrogen/component dilution respectively. The third flow controller (MFC-3), located prior to the injection manifold, meters the amount of the vapor mixture introduced into the reaction chamber. The pressure controller (PCV-1) maintains the desired pressure in the bubbler, which allows for repeatable mixing of the source vapor and the hydrogen carrier. Due to this system of gas

controls, the resultant gas flow from MFC-3 contains a desired amount of the particular source concentration. The separate source vapors, used to grow the desired material, are sent to the reaction chamber to thermally decompose onto the substrate, leading to growth of the desired material.

Since a change in vapor concentration results in a change in both the solid composition and growth rate, there is a clear need for a direct concentration measurement. Ideally the vapor concentration can be calculated, using tabulated vapor pressure data, for temperature, flows, and pressure used in the bubbler configuration. This calculation has potential for error as it assumes that the source bubbler is in thermodynamic equilibrium and that the temperature, flow, and pressure measurements are accurate. As shown in Fig. 1, the MOCVD system is equipped with an ultrasonic concentration sensor [9, 14]. With a direct sensor such as this, real-time control becomes possible.

Pure component flow expresses the amount of source vapor entering the reactor cell as a volume. Pure component flow (PCF) rate is the product of the precursor concentration and the corresponding mass flow rate into the reactor. This mass flow injected into the reactor consists of both the precursor vapor and the carrier gas. Hence, the goal is to obtain the desired PCF of each concentration-critical precursor throughout the entire growth, for example TMGa and TMIn when growing $Ga_xIn_{1-x}As$. The current method of obtaining the correct PCF is by pre-run calibration, where the source concentrations are measured before growth. The injection mass flow controller (MFC-3) set points are then programmed accordingly. During growth, however, the PCF is running in an open-loop fashion where there is no actuation responding to the concentration disturbances. Consequently, the desired

composition and thickness, and hence the resulting device performance, degrades due to the disturbances. On the contrary, a closed-loop system is one where signals containing disturbance information is used compensate for the disturbances and maintain the desired PCF.

Evidence of a TMIn concentration disturbance, which exhibits a time scale on the order of weeks, has been reported [9, 13] and compensated for by some groups [9, 12]. An example of a faster concentration disturbance is illustrated in Fig. 2(a), which is a plot of percent concentration of TMGa flowing in hydrogen, as measured by the concentration monitor during a normal growth run. Note that Fig. 2(a) represents concentration data for 10 minutes in the middle of a typical growth, and typical structures often require 30 minutes or longer. These concentration signal contains dynamics from a bubbler drift disturbance as well as the sensor noise. The drift disturbances are the components of the signal shown in Fig. 2(a) with the larger amplitudes and lower fluctuation frequencies. The sensor noise is the smaller amplitude, higher frequency component of the signal. To distinguish between the dynamics and noise, the hydrogen carrier gas alone was sent to the concentration sensor, bypassing the bubbler. A comparison of the two power spectra, shown in Fig. 2(b), provides evidence that in addition to sensor noise, the concentration signal illustrated in Fig. 2(a) is also corrupted by bubbler drift disturbances with energy in the 0.01-0.1 Hz frequency range; a range which can affect single layer growth. Several known factors contribute to this bubbler disturbance. First, the TMGa bath set point temperature is $-10°$ C, hence the thermodynamic stability of this source is very sensitive to environmental perturbations. Second, because the TMGa line is equipped with two mass flow controllers (MFC-1, MFC-2) and one pressure controller

(PCV-1) that affect the vapor concentration coming from the bubbler, the cumulative error from these three actuators is a significant source of disturbance for the vapor concentration.

One challenge in applying control to existing semiconductor processes is the selection and eventual retrofitting of transducers, both the actuators and the sensors. Figure 3 is a block diagram illustrating our chosen sensor, actuator, and other components of a single-source loop for PCF control. Based on this system block diagram, a model was developed to use in the controller synthesis [13]. As depicted in Fig. 3, the nominal concentration is corrupted by the concentration disturbance of the type shown in Fig. 2. The concentration measurement is also corrupted by sensor noise. The noise does not contain any useful information about the concentration signal and, when running in an open loop fashion, will not affect growth. The concentration disturbance, on the other hand, is real and will affect growth. It is important to note that once the loop is closed, the concentration sensor noise is part of the concentration signal being sent to the controller. Therefore, if the controller responds to the sensor noise, it will be harming the growth. Consequently, another controller design goal is to ignore or attenuate the sensor noise. The injected flow is corrupted by a switching disturbance at times when the reactants change in the injection manifold. The locations of the switching disturbance and the mass flow rate sensor noise were determined by the modeling process and are shown in Fig. 3. In this system there is no transducer that can measure the actual pure component flow, hence we construct the product of the measured concentration signal and the measured mass flow signal and define it to be the *observed* pure component flow, in lieu of a measured pure component flow.

The controller design objectives are nominal pure component flow regulation and disturbance

rejection. In control theory, a controller of this type is called a *regulator* because it governs a signal to remain constant in the presence of disturbances. As shown in Fig. 3, the controller input is the concentration monitor signal, and the controller output dynamically adjusts the MFC-3 actuator set point. This preliminary control strategy was first investigated for TMIn [9]. The controller structure simply divides the target pure component flow rate (PCF_{target}), as specified in required for the material, by the concentration signal (C_{meas}). The controller output is a flow rate set point (F_{set}) that satisfies

$$PCF_{target} = C_{meas} \times F_{set}.$$

This control law is simple, yet provides the necessary disturbance rejection.

The concentration signal was then filtered with a 0.1 Hz, 2-pole Butterworth filter to reduce the noise. The static nonlinear control law was implemented an analog divider circuit [15] and other analog components. The divider inputs included both the pure component flow reference signal (PCF_{target}) and the concentration sensor signal (C_{meas}). The output was the set point to the TMGa mass flow controller (F_{set}). A switch was installed to go between open and closed loop control.

2 Experimental Details

A multilayer structure was designed and grown to evaluate the control system. The structure grown consisted of alternating layers of InP and GaInAs, creating a superlattice. A superlattice was chosen for several reasons. First, the multilayers investigate composition at

defined stages of growth. Second, the superlattice nature acts as a probe to examine both the thickness and composition reproducibility from layer to layer [16]. The structure was grown under both open loop and closed loop conditions. During both growths the TMGa temperature was purposefully increased to cause a disturbance in the TMGa concentration. This temperature bath agitation was used to test the ability of the controller to reject large vapor concentration disturbances. After growth, samples were measured with a double-crystal X-ray diffractometer using Cu $K\alpha_1$ radiation and (004) reflection.

The growth first starts with a 1000 Å InP buffer layer grown on epi-ready InP (100) substrate, Fe doped, with a 2° vicinal misorientation towards [110]. The following GaInAs layer was grown to be nominally 3000 Å thick at a target growth rate of 14 Å/s. For the initial GaInAs layer, the TMGa was maintained at $-10°$ C. After the completion of the first GaInAs layer, a 200 Å InP spacer layer is grown at a growth rate of 2.7 Å. At the start of the spacer layer growth, the TMGa temperature bath set point was manually increased by 0.4° C. The spacer layer growth allows the TMGa to adjust to the new temperature. After the InP spacer growth, a blanket flow of TBP in hydrogen was sent to the reactor for 100 s to provide additional time for the TMGa bath to stabilize before the start of the growth of another 3000 Å GaInAs layer. The two-layer period of 200 Å InP/3000 Å GaInAs is repeated a total of four times, with a 0.4° C TMGa temperature increase after each GaInAs layer (cf., Table 1). The final structure provides five alloy layers as solid composition probes. Following these tests, a second set of open and closed loop growths were performed without inflicting a temperature disturbance to investigate the performance of the control system during regular growth. During all growths, the reactor pressure was 760 Torr and the sample temperature

was 645° C. For these experiments, the desired $Ga_xIn_{1-x}As$ composition is x = 0.47. For our growth conditions, a TMGa concentration of approximately 0.192 % (by volume) is injected at a flow rate of 90.6 sccm, resulting in a TMGa PCF rate of 0.174 sccm. This is equivalent to a molar flow rate of 7.8×10^{-6} moles per minute and an injected partial pressure of 24.7×10^{-3} Torr.

3 Results and Discussion

First, an agitated growth was performed to test the effectiveness of the controller. The experiment was structured to test the feasibility of the controller as well as investigate how well the control system can compensate for large amplitude perturbations. Time histories of performance parameters for the agitated growths are shown in Fig. 4. TMGa concentration signal from the concentration monitor, the flow measurement from MFC-3 on the TMGa line and the *observed* pure component flow of TMGa are compared for the open and closed loop growths. For each time history, 0 s marks the beginning of growth for the first GaInAs layer. The concentration of TMGa is shown to have five distinct levels corresponding to the five different set points in temperature (cf., Figs. 4(a) and 4(b)). The mean concentrations for each layer shown in Table 1 illustrate that the open and closed loop runs experienced similar concentration variations. Note the concentration response in Fig. 4(b) at approximately 200 s. The dip in concentration just before the end of the layer 1 growth is a transient caused by an air draft, which was generated when the access door was opened to adjust the temperature bath manual set point. This observation supports the belief that the bubbler

thermodynamics are extremely sensitive and the concentration can vary from environmental disturbances.

The output of the controller is a scaled inverse of the concentration measurement. Figures 4(c) and 4(d) are plots of the respective open and closed loop measured flow rates. As seen from Table 1, the open loop flow rate behaves as expected by remaining constant at approximately 90.6 sccm. The closed loop flow rate, however, decreases to compensate for the increasing concentration. Consequently, the open loop PCF varies, but the closed loop is regulated, as is illustrated in Figs. 4(e) and 4(f). These plots of the observed PCF were constructed by multiplying the sampled concentration signal data by the sampled injected flow signal data, where the concentration data was shifted by 2 s to compensate for the pipe transport delay. The key result in comparing the mean observed PCF values for each layer in Table 1 is that the closed loop system successfully regulated the PCF in the presence of the temperature agitation, whereas the open loop PCF was affected by the disturbance.

The control of solid composition and thickness from layer to layer was investigated with double crystal X-ray diffraction. Fig. 5 compares the rocking curves of the open and closed loop growths, for the experiment when the TMGa concentration was perturbed via the temperature bath. The open loop plot, shown in Fig. 5(a), contains one peak from the InP at an angle of zero arcsec and five overlapping peaks from the GaInAs layers at angles ranging from 50-500 arcsec. The closed loop plot, Figure 5(b), has one peak from the InP at an angle of zero arcsec and one peak from the GaInAs at 50 arcsec. The peak at 100 arcsec results from a satellite peak convolved with the zeroth order peak. From the compositional analysis for the $Ga_xIn_{1-x}As$ peaks, the resulting open loop composition varied from $0.475 \leq x \leq 0.5$,

while the closed loop composition was maintained at x = 0.473, in the presence of a similar concentration disturbance. Hence, the PCF control system has performed well, compensating for perturbations in real-time, and leading to a much improved multilayer sample.

The next set of growth experiments were designed to test the controller action during normal operation, with no imposed system disturbances. Figure 6 shows the rocking curves for open and closed loop growths. In superlattice structures, the presence of satellite peaks can be used as a measure of how well the thickness and composition of the periods are precisely repeated. The primary feature in the closed loop results, Fig. 6(b), which is evidence of an improved growth, is the presence of the eight orders of well-defined satellite peaks. This result indicates that in regulating the PCF rate of the gallium source, the growth rate and hence the thickness of the GaInAs layers were regulated, as well as the solid composition. Simulation of the X-ray diffraction spectra for the multilayer sample is shown as a dashed line in Fig. 6(b). In this simulation, the alloy composition was kept constant throughout each layer and also in each of the five layers. The match between the simulation of the nominal structure and the actual measurement further confirms the ability of the controller to improve reproducibility from layer to layer, a major requirement in superlattice growth.

4 Summary

Future advances in the epitaxial growth of semiconductors will require real-time sensing of key parameters and, where possible, real-time automated control of these parameters. To address these objectives, we developed a controller that uses an ultrasonic concentration sen-

sor to provide real-time information about the TMGa gas concentration during the growth of GaInAs by MOCVD. Steps in control system development include identifying and characterizing a disturbance that compromises sample quality, designing a control law to regulate the disturbance, and implementing the controller with appropriate hardware. We devised a simple law to maintain the PCF of the TMGa in the presence of concentration disturbances and implemented it with a analog circuit that controls the injection mass flow controller. A GaInAs/InP superlattice with thick alloy layers was characterized by X-ray diffraction to evaluate both the resulting thickness and solid composition variations that occurred from layer to layer and within a layer. The controller rejected intentional large amplitude concentration perturbations present during growth, resulting in a superlattice of moderate quality. The controller also vastly improved a sample grown during unperturbed growth, leading to a high quality superlattice. These results demonstrate that our specific implementation has the ability to improve the precision and reproducibility of solid composition and layer thickness - both primary features in the epitaxy of high performance semiconductor devices.

Acknowledgements

The authors would like to thank Trevor Grantham and John Crawley for useful discussions. The instrumentation, and a part of the control work was supported by the ARPA Optoelectronic Technology Center (OTC) under contract MDA 972–94–1–0002. The work of C. Reaves was supported by the NSF Science and Technology Center for Quantized Electronic Structures (QUEST) under contract number DMR 91–20007. The work of M. Gaffney

and R. Smith was supported in part by NSF under contract ECS-93-8917.

References

[1] J.D. Stuber, I. Trachtenberg, T.F. Edgar, J.K. Elliot, and T. Breedijk, Proc. IEEE Control Decision Conf. (1994) 79.

[2] A. Emami-Naeini, M.G. Kabuli, and R.L. Kosut, Proc. 33rd IEEE Conf. Decis. Contr. (1994) 73.

[3] S.W. Butler, K.J. McLaughlin, T.F. Edgar, and I. Trachtenberg, J. Electrochem. Soc. 138 (1991) 2727.

[4] T.L. Vincent, P.P. Khargonekar, B.A. Rashap, F. Terry, and M. Elta, Proc. Amer. Control Conf. 1 (1994) 902.

[5] L. Layeillon, A. Dollet, J.P. Couderc, and B. Despax, Plasma Sources, Science & Tech. 3 (1994) 72.

[6] G.P. Agrawal and N.K. Dutta, Semiconductor Lasers, 2nd ed. (Van Nostrand Reinhold, New York, 1993).

[7] J. Blondelle, H. De Neve, P. Demeester, P. Van Daele, R. Baets, and G. Borghs, presented at the Sixth European Workshop on Metal-Organic Vapour Phase Epitaxy and Related Growth Techniques in Gent, Belgium (1995).

[8] G. Bastard, Appl. Phys. Lett. 43 (1983) 591.

[9] J.P. Stagg, J. Christer, E.J. Thrush, and J. Crawley, J. Crystal Growth 120 (1992) 98.

[10] D.E. Aspnes, Proc. Conf. on Indium Phosphide and Related Materials (1994) 292.

[11] N. Kobayashi, J. Crystal Growth 145 (1994) 1.

[12] R.M. Biefeld and S.R. Kurtz, submitted to the J. Electron. Mater. (1995).

[13] M.S. Gaffney, R.S. Smith, A.L. Holmes, Jr., C.M. Reaves, and S.P. DenBaars, Proc. 34th IEEE Conf. Decis. Contr. (1995).

[14] EPISON, manufactured under license from Northern Telecom Europe Limited by Thomas Swan and Co. Ltd., Semiconductor Division, Unit 1C, Button End, Harston, Cambridge, CB2 5NX, UK.

[15] Internally Trimmed Precision IC Multiplier, AD534, manufactured by Analog Devices.

[16] V. Swaminathan and A.T. Macrander, Materials Aspects of GaAs and InP Based Structures (Prentice Hall, Englewood Cliffs, NJ, 1991).

[17] M.S. Gaffney, C.M. Reaves, R.S. Smith, A.L. Holmes, Jr., and S.P. DenBaars, accepted for the 13th World Congress IFAC (1996).

Table 1: Comparison of mean TMGa concentration measurement, flow measurement, and pure component flow observation during GaInAs growth. Note that the observed PCF in the closed loop case is the same for all layers. The TMGa source bath temperature set point is shown for each layer.

Layer	Temp. (° C)	Mean Concentration (% by volume)		Mean Flow (sccm)		Mean Observed PCF (sccm)	
		Open Loop	Closed Loop	Open Loop	Closed Loop	Open Loop	Closed Loop
1	-10.0	0.191	0.190	90.6	90.4	0.173	0.172
2	-9.6	0.196	0.195	90.6	87.6	0.178	0.171
3	-9.2	0.199	0.199	90.6	86.7	0.180	0.172
4	-8.8	0.204	0.204	90.6	84.0	0.185	0.171
5	-8.4	0.209	0.209	90.6	82.0	0.189	0.171

Figure Captions

Fig. 1: Simplified schematic overview of the MOCVD process for one source (TMGa). Mass flow controllers: MFC-1, MFC-2, MFC-3. Pressure controller: PCV-1. Ultrasonic concentration monitor located on the output of PCV-1. Gas flow directions shown by arrows. Manifold switching and hand valves not shown.

Fig. 2: Concentration variation of TMGa during a typical growth measured in percent by volume of injected gas is shown in (a). The target concentration is shown by a dashed line. To distinguish between bubbler disturbances and concentration sensor noise, the power spectra of this data is shown in (b) as a solid line. For comparison, the power spectra of only hydrogen concentration measurements (bypassing the bubbler) is shown as a dash-dot line in (b). Note the higher energy in the TMGa spectra at frequencies less that 0.1 Hz.

Fig. 3: Block diagram of the pure component flow control system model. The observed pure component flow is the product of the measured concentration signal and the measured mass flow signal. This step is indicated by the block containing "X".

Fig. 4: Open and closed loop TMGa responses to temperature bath agitation. Shaded regions indicate growth of GaInAs layers. The TMGa concentration time histories are compared in (a) open loop and (b) closed loop. The flow rate time histories (measurement located at the injection flow controller) are compared in (c) open loop and (d) closed loop. The corresponding observed pure component flow time histories are compared in (e) open loop and (f) closed loop.

Fig. 5: X-ray diffraction rocking curves from GaInAs/InP superlattices grown with the TMGa temperature bath agitation for (a) open and (b) closed loop growths.

Fig. 6: X-ray diffraction rocking curves from GaInAs/InP superlattices grown in normal operation for (a) open and (b) closed loop growths. Solid lines indicate measurement; dashed line in (b) indicates simulation results.

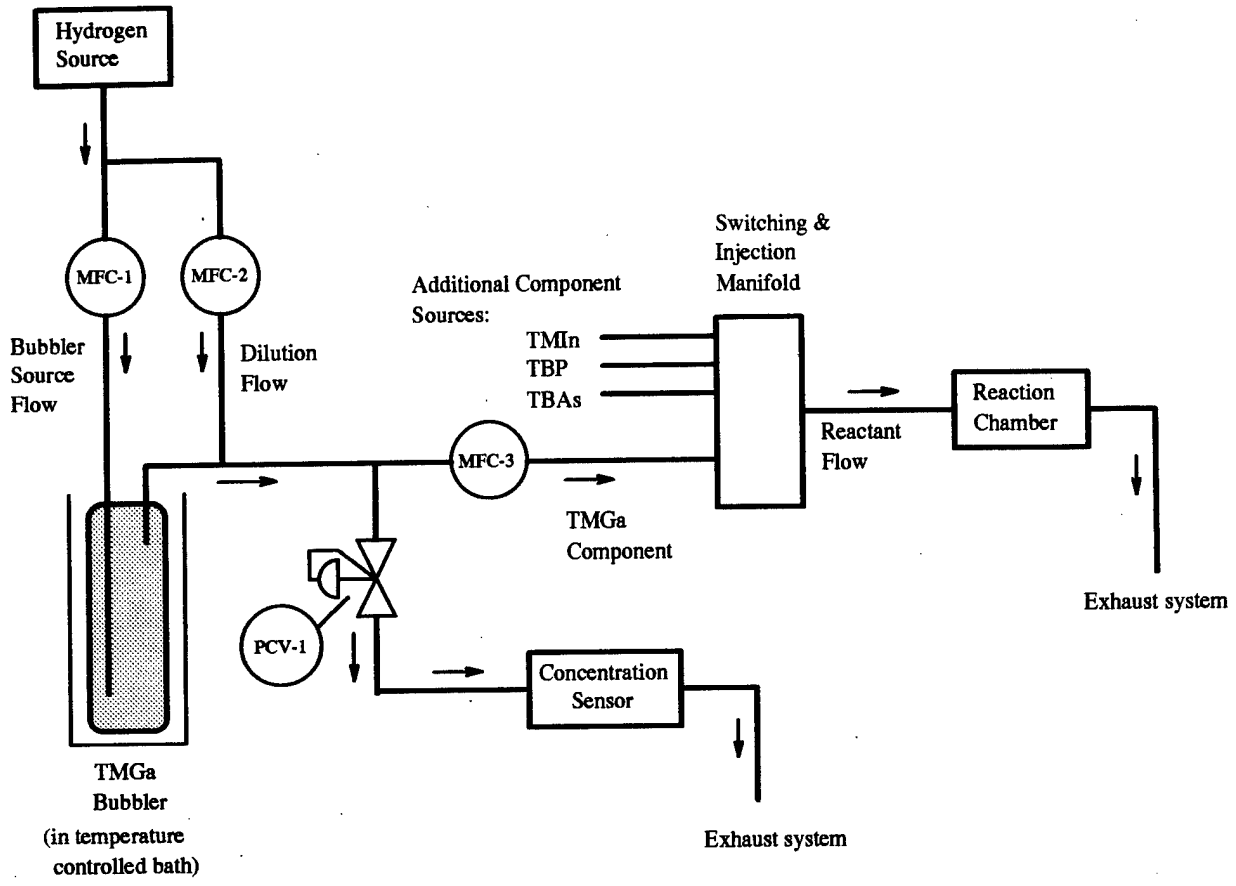
Hydrogen Source
MFC-1
MFC-2
Bubbler Source Flow
Dilution Flow
Additional Component Sources:
TMIn
TBP
TBAs
Switching & Injection Manifold
Reaction Chamber
Reactant Flow
MFC-3
TMGa Component
Exhaust system
PCV-1
Concentration Sensor
TMGa Bubbler (in temperature controlled bath)
Exhaust system

Figure 1

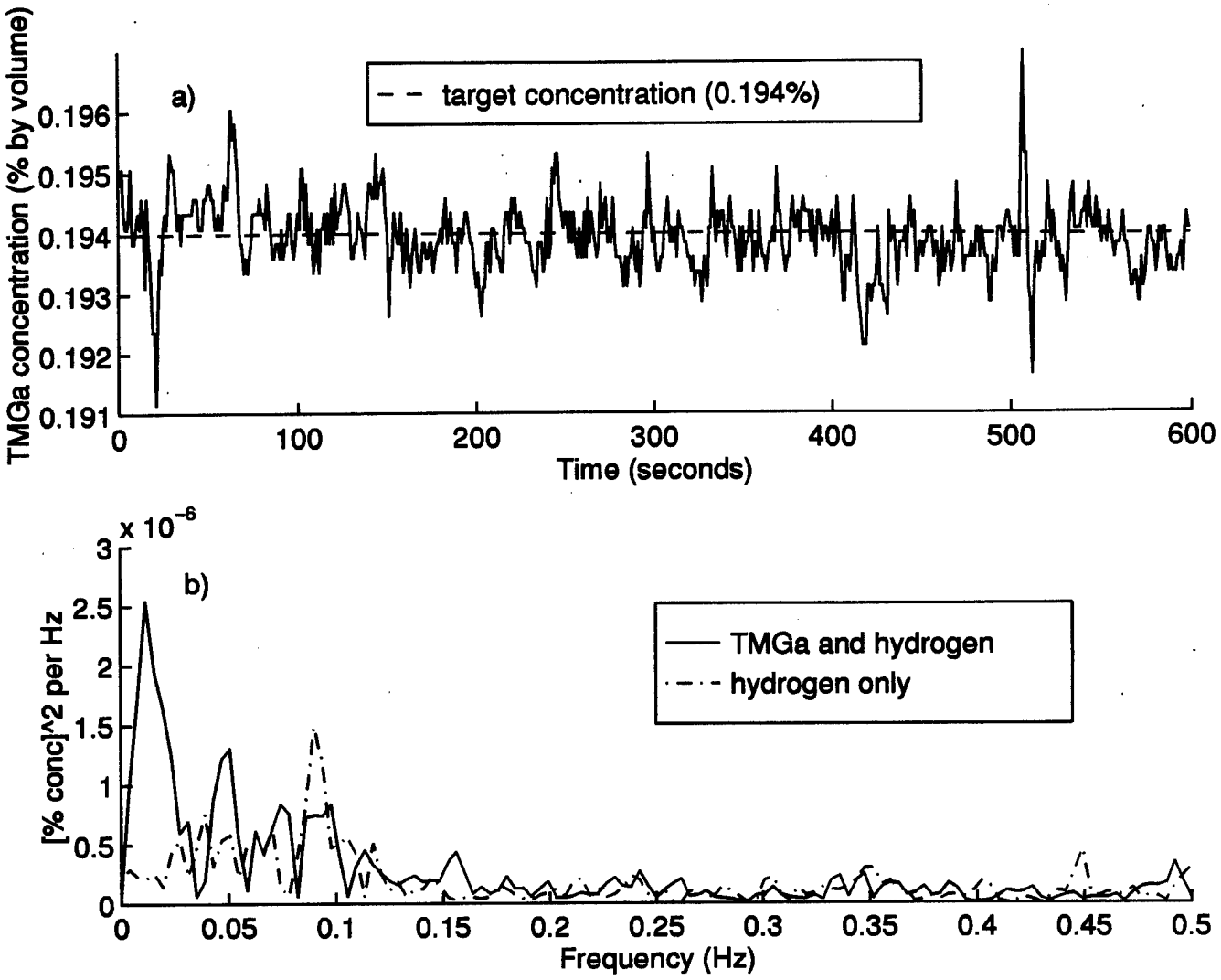
a)
target concentration (0.194%)
TMGa concentration (% by volume)
0.196
0.195
0.194
0.193
0.192
0.191
0
100
200
300
400
500
600
Time (seconds)

x 10^-6
b)
TMGa and hydrogen
hydrogen only
[% conc]^2 per Hz
3
2.5
2
1.5
1
0.5
0
0
0.05
0.1
0.15
0.2
0.25
0.3
0.35
0.4
0.45
0.5
Frequency (Hz)

Figure 2

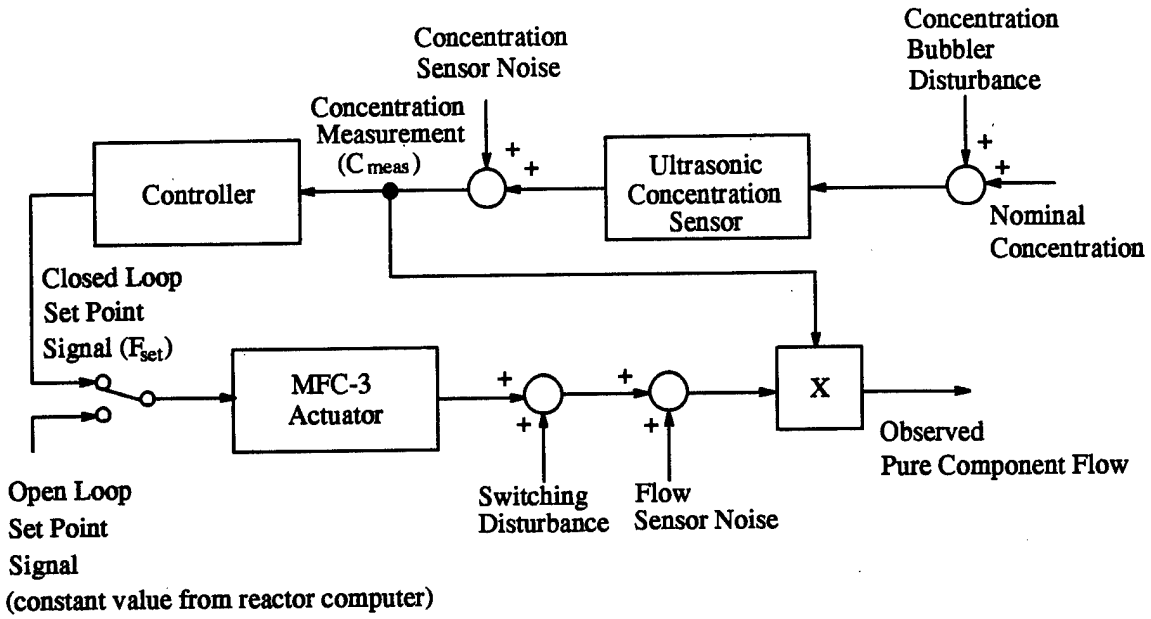
Concentration
Sensor Noise
Concentration
Bubbler
Disturbance
Concentration
Measurement
(C meas)
Controller
Ultrasonic
Concentration
Sensor
Nominal
Concentration
Closed Loop
Set Point
Signal (F set)
MFC-3
Actuator
X
Observed
Pure Component Flow
Open Loop
Set Point
Signal
(constant value from reactor computer)
Switching
Disturbance
Flow
Sensor Noise

Figure 3

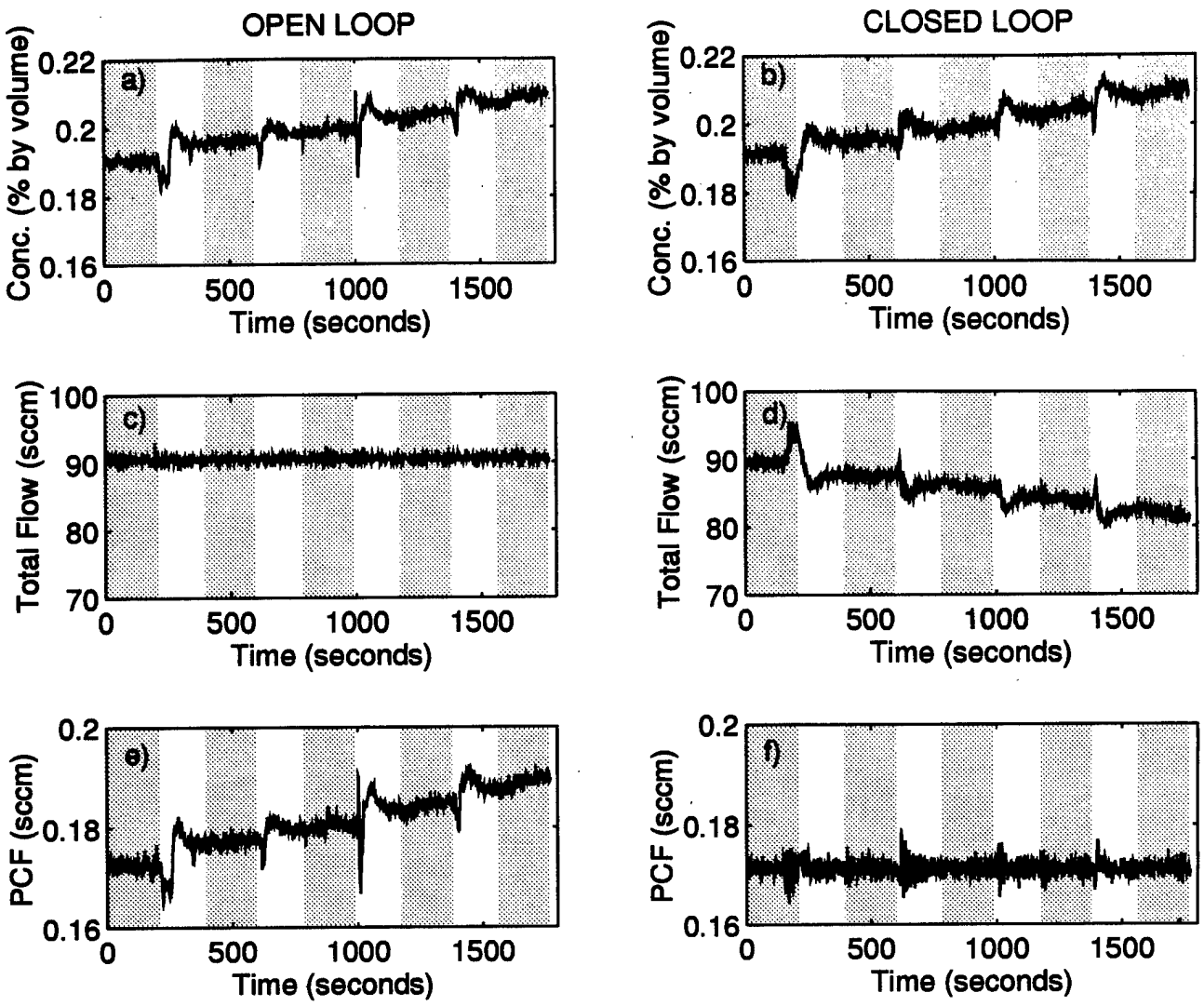
OPEN LOOP
CLOSED LOOP
a)
b)
c)
d)
e)
f)
Conc. (% by volume)
Total Flow (sccm)
PCF (sccm)
Time (seconds)
0.22
0.2
0.18
0.16
100
90
80
70
0
500
1000
1500

Figure 4

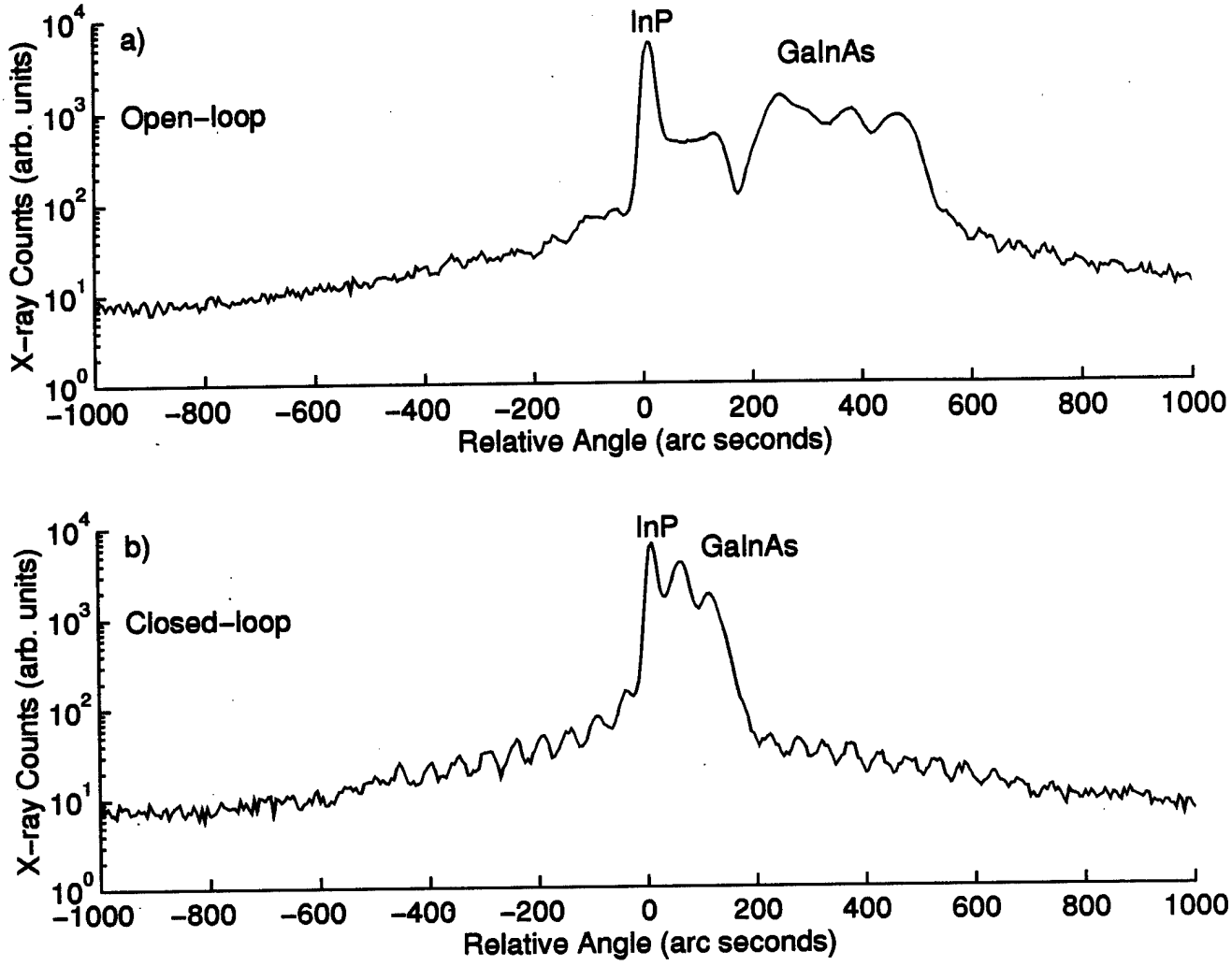
a)
Open–loop
InP
GaInAs
X–ray Counts (arb. units)
Relative Angle (arc seconds)
b)
Closed–loop
InP
GaInAs
X–ray Counts (arb. units)
Relative Angle (arc seconds)

Figure 5

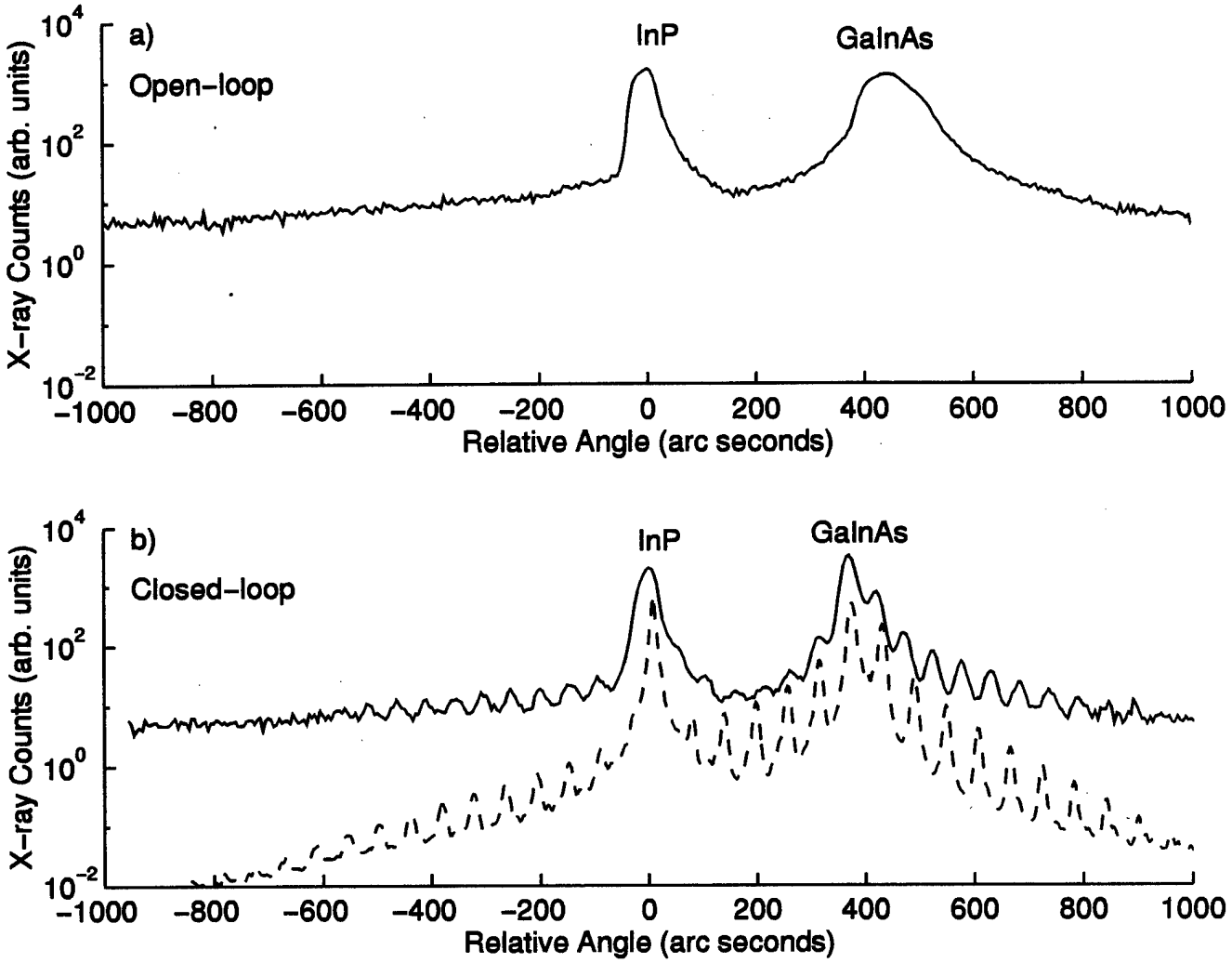
a)
Open-loop
InP
GaInAs
X-ray Counts (arb. units)
10^4
10^2
10^0
10^{-2}
−1000 −800 −600 −400 −200 0 200 400 600 800 1000
Relative Angle (arc seconds)
b)
Closed-loop
InP
GaInAs
X-ray Counts (arb. units)
10^4
10^2
10^0
10^{-2}
−1000 −800 −600 −400 −200 0 200 400 600 800 1000
Relative Angle (arc seconds)

Figure 6

M. Gaffney, C. M. Reaves, A. L. Holmes, Jr., R. Smith, and S. P. DenBaars, "Real-time composition and thickness control techniques in a metalorganic chemical vapor deposition process," in *Symposium on Diagnostic Techniques for Semiconductor Materials Processing* (S. W. Pang, ed.), vol. 406, Mater. Res. Soc., 1995.

REAL-TIME COMPOSITION AND THICKNESS CONTROL TECHNIQUES IN A METALORGANIC CHEMICAL VAPOR DEPOSITION PROCESS

M.S. Gaffney[†,*], C.M. Reaves[‡], A.L Holmes, Jr.[†], R.S. Smith[†], S.P. DenBaars[‡,†]
Departments of Electrical and Computer Engineering[†] and Materials[‡]
University of California, Santa Barbara, CA 93106
*gaffney@seidel.ece.ucsb.edu

ABSTRACT

Metalorganic chemical vapor deposition (MOCVD) is a process used to manufacture electronic and optoelectronic devices that has traditionally lacked real-time growth monitoring and control. We have developed control strategies that incorporate monitors as real-time control sensors to improve MOCVD growth. An analog control system with an ultrasonic concentration monitor was used to reject bubbler concentration disturbances which exist under normal operation, during the growth of a four-period GaInAs/InP superlattice. Using X-ray diffraction, it was determined that the normally occurring concentration variations led to a wider GaInAs peak in the uncompensated growths as compared to the compensated growths, indicating that closed loop control improved GaInAs composition regulation. In further analysis of the X-ray diffraction curves, superlattice peaks were used as a measure of high crystalline quality. The compensated curve clearly displayed eight orders of satellite peaks, whereas the uncompensated curve shows little evidence of satellite peaks.

INTRODUCTION

Stricter semiconductor device tolerance requirements [1, 2, 3] are driving the need for better monitoring and control in semiconductor fabrication processes. Metalorganic chemical vapor deposition (MOCVD) is a widely used technique for epitaxial growth of semiconductor layers, but is limited by a high degree of process variance. Recently, the MOCVD process has been improved with real-time closed loop control [4, 5], using a concentration monitor. In previous work [5], a control system was designed to improve both epitaxial thickness and composition precision. The controller is designed to maintain a constant delivery rate of one component of the semiconductor alloy being grown in the reactor. The primary goal of this paper is to outline general procedures for the design and implementation of a control system for epitaxial growth. A secondary goal consists of describing the control system implementation and a growth demonstration. To achieve these goals, the paper contains a brief overview of the system and experiment, followed by a detailed discussion of the control issues.

SYSTEM OVERVIEW

Metalorganic chemical vapor deposition (MOCVD) is a vapor-phase growth technique used to grow a wide range of semiconductors and other materials. Fig. 1 is a schematic overview of the MOCVD delivery system for a single source. The atoms that are needed to create the thin films found in single-crystal compound semiconductors are supplied from precursors that can be solid, liquid, or gas. In the case of solid and liquid precursors, the vapor that arises from evaporation is transported to the reaction chamber by passing hydrogen gas (or another pure carrier gas) through the source vessel that stores the liquid or

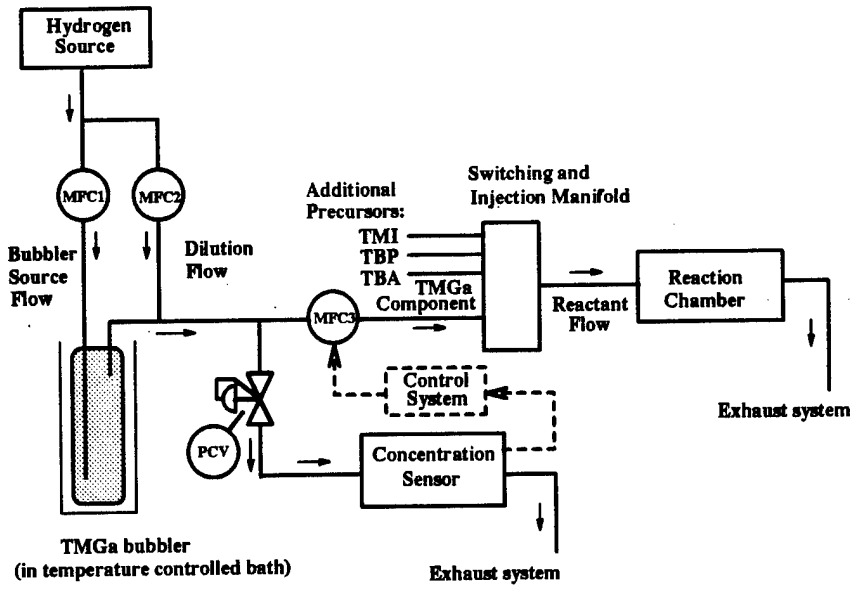

Figure 1: Simplified schematic overview of the MOCVD process for one source (TMGa). Mass flow controllers: MFC1, MFC2, MFC3. Pressure controller: PCV. Manifold switching and hand valves not shown. Gas flow directions shown by arrows. Location of control system is indicated with dashed lines.

solid precursor. The resulting gas flow from the bubbler consists of hydrogen and the source vapor. This mixture is transported to the reaction chamber where the crystal growth occurs.

Obtaining the desired concentration of the source vapor in the gas flow is critical for precise growth. For control of the solid composition and thickness of an alloy layer, the primary parameters of interest include the relative amounts of precursor vapor entering the reaction chamber. This is due to the fact that MOCVD growth of III-V semiconductors is often performed in a regime where the amount of source vapor determines how many atoms of a particular element is incorporated into a film. To achieve the desired amount of the source vapor, the transport system is configured with several key features [5]. The desired precursor concentration, for example trimethylgallium (TMGa), is obtained by a system of mass flow controllers (MFC1, 2, and 3) and a pressure controller (PCV). The system is also equipped with a concentration sensor, which is used to measure the percent concentration of the precursor in hydrogen, and is located on a bleed line after MFC2, but before MFC3.

Ultimately in MOCVD, the primary growth parameter for solid composition and thickness control is the source vapor delivery to the growth chamber. One common way to express the amount of vapor entering the reactor cell is by pure component flow. Pure component flow (PCF) rate is the product of the precursor concentration and the corresponding mass flow rate into the reactor. This flow into the reactor consists of both the precursor vapor and the carrier gas, and hence is termed the total flow (for one source line). The present practice for obtaining the pure component flow is by pre-growth calibration with the concentration monitor. Before growth, the injection mass flow controller (MFC3) is set to a flow rate value where the product of the total flow rate and the pre-run concentration reading is the desired pure component flow. The drawback to this open-loop method is that bubbler concentration disturbances, characterized in [5], will perturb both the desired composition and thickness in the growth. These disturbances, primarily from the TMGa bubbler, have time scales that affect uniformity between layers and even within single layer. The ultrasonic concen-

tration sensor, previously mentioned, can detect these disturbances that perturb growth in a real-time therefore is used in the control loop.

EXPERIMENT

Fig. 1 illustrates the control system (dashed line) that uses the concentration signal from the sensor as the control input, and continuously adjusts the total flow rate set point of the injection mass flow controller (MFC3), in order to maintain a constant pure component flow rate. The controller objectives are nominal TMGa pure component flow regulation and disturbance rejection (remembering that the pure component flow is the product of the component concentration and total flow). The controller structure, first investigated by Stagg, *et al.*, [4] for TMI, simply divides the target pure component flow rate (PCF_{target}), as required for the particular growth, by the concentration sensor signal (C_{meas}). The controller output, therefore, is a mass flow rate set point (F_{set}) that satisfies the PCF control law,

$$PCF_{target} = C_{meas} \times F_{set}. \tag{1}$$

Once a control law is developed it must be implemented with hardware. The initial controller implementation was fabricated with analog components and is illustrated in Fig. 2. Retrofitting the control system to the existing MOCVD machine, while not disturbing the ongoing open loop growth capabilities, was a design priority. The concentration signal was taken into a high impedence buffer so as to not affect the sensor performance. The concentration signal was then filtered with a 0.1 Hz, 2-pole Butterworth filter to reduce the noise and also prevent the controller from responding to erroneous concentration monitor signals. The static nonlinear control law, Eq. 1, was implemented via an divider circuit [6] and other analog components. The divider chip inputs included both the pure component flow reference signal (PCF_{target}) and the concentration sensor signal (C_{meas}). The output was the set point to the TMGa injection mass flow controller (F_{set}). A switch was installed to select either open or closed loop control. Open loop control signifies that the mass flow controller set point signal is generated from the MOCVD reactor computer, and will not change as a function of the concentration signal. Closed loop control signifies that the set point is generated from the analog implementation.

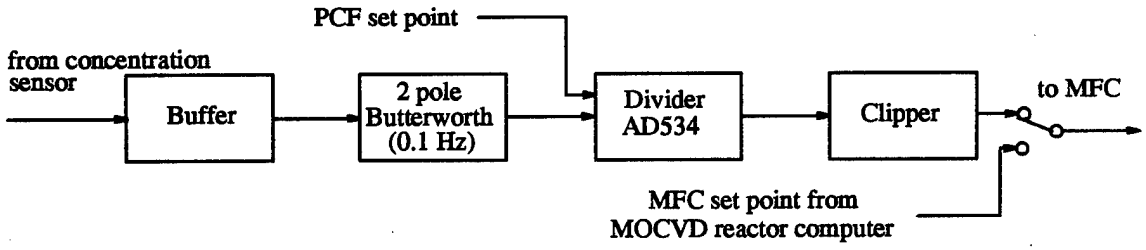

Figure 2: Block diagram of the controller implementation. The input is the concentration sensor signal and the output is the mass flow controller set point.

A multilayer structure was designed to examine the controller performance in regulating both the composition and thickness of the GaInAs layers and is shown in Fig. 3. This superlattice-like structure was chosen to investigate the control system reproducibility action. During growth, the reactor pressure was 760 Torr and the sample temperature was 645° C. The substrates were epi-ready InP(100), Fe doped, with a 2 ° vicinal misorientation.

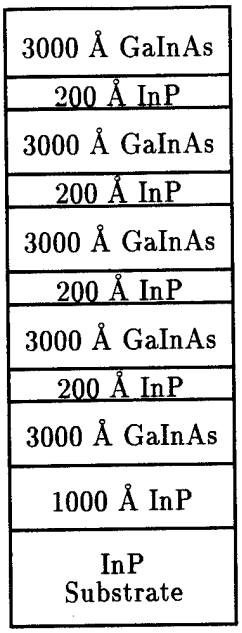

Figure 3: Experimental growth structure designed to test the controller performance. Note the four periods GaInAs/InP (3000 Å/200 Å) superlattice structure.

The structure shown in Fig. 3 was growth under both open and closed loop conditions for comparison.

The solid composition and thickness control was measured with a double-crystal X-ray diffractometer using Cu $K\alpha_1$ radiation and (004) reflection. Fig. 4 compares X-ray rocking curves for the open and closed loop growths of the test structure. Improved solid composition control is evident from the reduced width of the closed loop GaInAs lattice peak (note that this peak is convoluted with satellite peaks). In addition to composition control, the thickness reproducibility also improved with the closed loop controller. The compensated growth contains eight orders of well-defined satellite peaks [5], indicating that a constant thickness of the repeated GaInAs layers has been maintained. The lack of satellite peaks in the open loop curve shows evidence that the bubbler concentration disturbances corrupt thickness reproducibility. The dashed line in Fig. 4 is a diffraction simulation of the test structure shown in Fig. 3. The match between simulation and closed loop data supports the success of control system in improving layer-to-layer reproducibility.

DISCUSSION OF CONTROLLER DESIGN ISSUES

The control system synthesis to improve the precision in MOCVD, involves several overlapping procedures. A desired performance improvement must be identified along with the performance limiting factors that can be potentially bettered by a control system. For vapor phase epitaxy, improved precision in both thickness and composition are desirable, however the accuracy of the vapor concentration delivery limits the thickness and composition tolerances. Once a desired improvement and limiting factors are specified, a control loop,

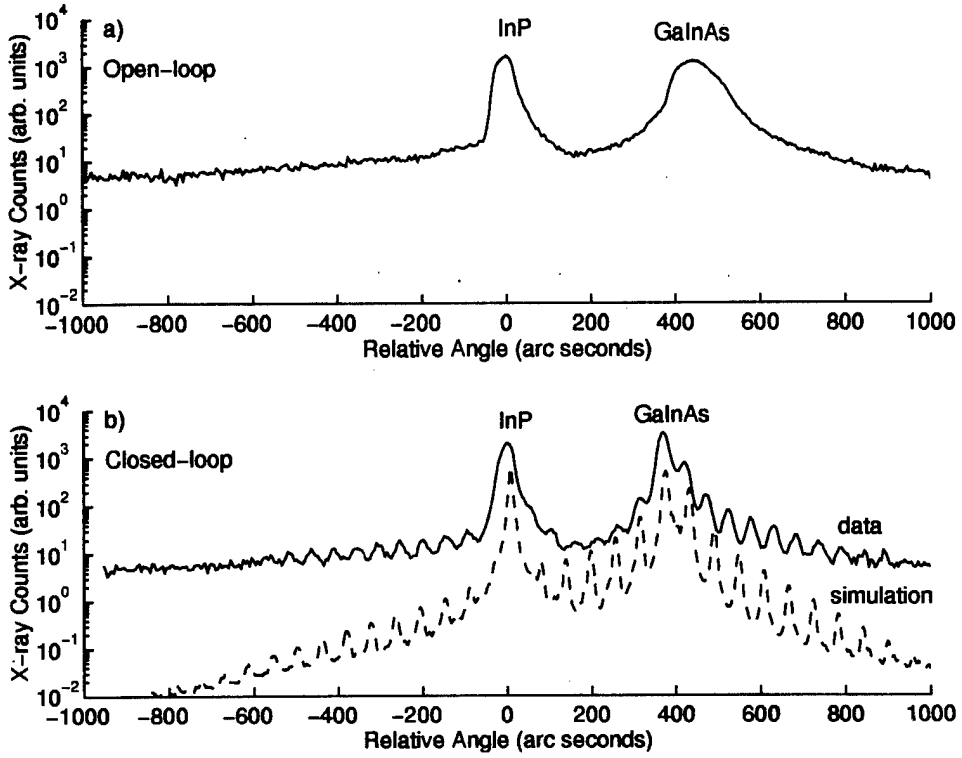

Figure 4: X-ray diffraction rocking curves for (a) open and (b) closed loop growths in normal operation. The dashed line indicates results from a simulation.

including both sensors and actuators, must be defined. As an alternative to the control actuator MFC3, the dilution mass flow controller (MFC2 in Fig. 1) could have been chosen to reject disturbances, but the control law would then differ. The limiting factors on performance often manifest themselves as system disturbances, as in the vapor concentration fluctuations from the bubbler. Consequently, one consideration is what sensors are available to monitor the disturbances. For pure component flow control, the ultrasonic concentration monitor measured, in real-time, some evidence of the bubbler variability [5] and, hence, was a useful sensor in the loop.

The next step in the design procedure is to model the control loop and study the closed-loop behavior of the system [7]. Simple oversights, such as the physical limitations of actuators or unexpected sensor noise amplification, may cause problems when closing the loop, and therefore should be investigated with a model and simulation. Typically, a control loop model contains mathematical descriptions for the sensor, actuator, and process dynamics, as well as characterizations of the system disturbances. Characterizing a disturbance consists of determining where the disturbance enters the loop as well as what dynamics and noise signals make up the disturbance. Descriptions for the concentration sensor and MFC actuator, and characterizations of the concentration bubbler disturbance, switching disturbance, and sensor noise disturbances were determined by recording responses to known inputs [7]. The sensor response was analyzed to determine which components of the signal were sensor noise and which showed evidence of the bubbler variability. During the controller design, both hardware selection and installation issues should be considered. For pre-existing MOCVD systems, retrofitting a controller may hinder the controller performance due to the fact that

the sensor and actuator configuration was not designed for feedback.

Specific experimental growths must also be designed in order to examine the performance of the controller. Often in semiconductor fabrication, the only way to determine if the controller is successful is by growing and then characterizing a series of samples. Our test structure can be characterized by X-ray diffraction, as shown Fig. 4, or by optical techniques. If the structure is also a superlattice, the satellite peaks can provide additional information about thickness and compositional uniformity of the sample. The ability to simulate the X-ray diffraction of such structures is a powerful method to evaluate the performance of a control system in addressing small time-scale variations.

CONCLUSIONS

By performing key control system design steps described above, we have built a successful real-time control implementation to reduce MOCVD processing variance. A vapor concentration monitor was used as the control input to detect TMGa concentration disturbances. A control law, designed to regulate the pure component flow of TMGa, adjusted the total mass flow rate set point of the TMGa in a hydrogen carrier. The performance objective was to improve both solid composition and thickness precision in the presence of normally occurring concentration fluctuations. The controller success, in regulating of both composition and thickness, was demonstrated by growing a four period GaInAs/InP superlattice and analysing both open and closed loop samples with X-ray diffraction techniques. The closed loop rocking curve had a narrower GaInAs peak and exhibited well defined satellite peaks as compared to the open loop rocking curve, indicating better composition and thickness precision.

ACKNOWLEDGMENTS

The authors would like to thank Trevor Grantham and John Crawley of Thomas Swan & Co., Ltd. for useful discussions. The instrumentation and a part of the control work was supported by the ARPA Optoelectronic Technology Center under contract MDA 972–94–1–0002. The work of C. Reaves was supported by the NSF Science and Technology Center for Quantized Electronic Structures under contract number DMR 91–20007. The work of M. Gaffney and R. Smith was supported in part by NSF under contract ECS-93-8917 and the Ralph M. Parsons Foundation.

REFERENCES

1. J. Blondelle, H. De Neve, P. Demeester, P. Van Daele, G. Borghs, and R. Baets, Electron. Lett., **31**, 1286 (1995).
2. G. P. Agrawal and N. K. Dutta, Semiconductor Lasers, 2nd ed. (Van Nostrand Reinhold, New York, 1993).
3. G. Bastard, Appl. Phys. Lett., **43**, 591 (1983).
4. J. Stagg, J. Christer, E. Thrush, and J. Crawley, J. Cryst. Growth, **120**, 98 (1992).
5. M. S. Gaffney, C. M. Reaves, R. S. Smith, A. L. Holmes, Jr., and S. P. DenBaars, J. Cryst. Growth, In revision.
6. Internally Trimmed Precision IC Multiplier, AD534, Analog Devices.
7. M. S. Gaffney, R. S. Smith, A. L. Holmes, Jr., C. M. Reaves, and S. P. DenBaars, accepted for the 34th IEEE Conference on Decision & Control, Dec. 1995.

M. S. Gaffney, C. M. Reaves, R. S. Smith, A. L. Holmes, Jr., and S. P. DenBaars, "Modeling and control of a metalorganic chemical vapor deposition process for III-V compound semiconductor epitaxy." To be presented at the 13th World Congress IFAC, July 1996.

Modeling and Control of a Metalorganic Chemical Vapor Deposition Process for III-V Compound Semiconductor Epitaxy[1]

Monique S. Gaffney*, Casper M. Reaves, Archie L. Holmes, Jr.*, Steven P. DenBaars*,** and Roy S. Smith***

*Department of Electrical & Computer Engineering, University of California, Santa Barbara, CA 93016. USA (M. Gaffney: +1 805 893-7785. gaffney@seidel.ece.ucsb.edu or R. Smith: +1 805 893-2967. roy@ece.ucsb.edu)

**Department of Materials, University of California, Santa Barbara, CA 93106. USA

Abstract. Real-time control of metalorganic chemical vapor deposition (MOCVD) processes has been shown to improve the composition and thickness precision in the growth of compound semiconductor films. A system model of the MOCVD process is developed to improve the application of control. The model is used to simulate growth of GaInAs. Estimates of the GaAs fraction, from simulated growths, are compared to measured composition results. The model estimates and post-growth data are in good agreement.

Key Words. compound semiconductor control, ultrasonic transducer

1. INTRODUCTION

One leading epitaxy technique used to grow compound semiconductors is metalorganic chemical vapor deposition or MOCVD. Compound semiconductor devices, such as electron mobility transistors, quantum-well lasers, and high brightness light emitting diodes (LEDs), are used in high speed computing and telecommunications applications. As the specifications for semiconductor materials and devices become more demanding, the precision and reproducibility capabilities in MOCVD technologies must be improved. In particular, the composition and thickness of layers within a device are parameters that possess extremely tight product tolerances. Examples of composition and thickness device specifications can be found in Agrawal and Dutta (1993), Blondelle et al., (1995), and Bastard (1983). As of late, epitaxial processes are becoming equipped with monitoring systems to sense the growth parameters of interest, such as sample temperature, layer thickness, state of the sample surface, and vapor concentration. The next step for MOCVD technology is to further develop these monitoring capabilities and incorporate them into a control system framework (Stagg et al., 1992; Aspnes et al., 1992; Koybayashi 1994; Biefeld and Kurtz 1995; Gaffney et al., 1995a,b).

MOCVD processes have much to gain from controller implementations because these processes are predominately run in an open loop fashion. For many systems, calibrations and adjustments are made before a run or by an operator during a run. By using process monitoring, these adjustments can be controlled in real time and with extreme precision. As was shown in Gaffney et al., (1995a,b), successful controller performance, leading to process improvements, can be obtained with simple control designs. The key control issues for the MOCVD system are not found in the control law design, but rather in the sensor technologies, disturbance identification, system analysis using a control-type model, and controller performance evaluations schemes.

This paper begins with a brief review of the MOCVD process and a discussion of recent closed loop control results found in Gaffney et al., (1995a,b). The primary motivation of this paper however, is to introduce a system model of the MOCVD process. The purpose of this model is to evaluate various sensor/actuator configurations, test controller designs, identify locations for new sensing schemes and estimate both composition and growth rate parameters. In this paper, the model is first described, then tested by driving a simulation with time history data taken from both open loop and closed loop

[1] This work was supported by NSF grant ECS-9308912. The work of M. Gaffney was supported, in part, by the Ralph M. Parsons Foundation. The work of C. Reaves was supported by the NSF Science and Technology Center for Quantized Electronic Structures (QUEST). The instrumentation was supported by the ARPA Optoelectronic Technology Center (OTC) under contract MDA 972-94-1-0002.

GaInAs (gallium indium arsenide) growths. The simulation performance, in estimating the composition x of $Ga_xIn_{(1-x)}As$, is compared with corresponding post-growth X-ray diffraction composition measurements.

2. CONTROL OF MOCVD PROCESS

2.1. *Background and Motivation*

The following description is a brief summary of the system overview contained in Gaffney et al., (1995a,b) MOCVD is one technique used to grow compound semiconductors (Dupuis 1984). An example of ternary MOCVD growth is when two column III alkyl sources, such as trimethylgallium (TMG) and trimethylindium (TMI), are mixed in a vapor phase with an organometalic column V source, such as tertiarybutylarsine (TBA). Under specific conditions, including reactor pressure, temperature, and molar flow rates, the deposition of a solid will occur. For TMG, TMI, and TBA, the resulting solid is $Ga_xIn_{(1-x)}As$. In III-V growth, the column III and V atoms primarily deposit in a 1:1 ratio. The column III ratio x, in the ternary compound example, is one of two main parameters to control. This molar ratio, or composition, has tolerances of $\pm$ 0.01 in order to obtain the desired emission wavelength from a quantum-well laser for example. The thickness or growth rate is the other parameter which must obtained precisely in the fabrication of electronic-grade devices.

Figure 1 is an overview of the gas flow through the system for a single source. The source chemicals are transported to the growth chamber in a vapor phase by bubbling hydrogen gas through the source vessel that stores the liquid reagent. This vessel is referred to as a bubbler. The resulting gas flow from the bubbler consists of hydrogen and the desired concentration of the source. The source concentration is regulated by three mass flow controllers, the input controller located before the bubbler (MFC3), an H_2 dilution controller located after the bubbler (MFC2), and the last one located before the injection manifold (MFC1) and a pressure controller (PCV1).

In the reaction chamber, a susceptor is heated by IR lamps and holds the substrate where growth occurs. The precursors, both the column IIIs and Vs, decompose at the hot surface. For the desired crystal growth to occur, the column III reagent compositions sent to the reactor are precise quantities, while the column V compositions are present in an overabundance. After a growth, information about the resulting composition and thicknesses can be determined using X-ray diffraction techniques.

In mass-transport limited MOCVD processes, both composition and growth rate (thickness) are proportional to the delivery rate of the column III precursors. The key parameter is the pure component flow rate, which is the product of the concentration of the source in the hydrogen carrier multiplied by the total flow rate of the source in the carrier. The typical growth procedure involves measuring the concentration of the ultrasonic concentration monitor before growth, and then adjusting the mass flow controller located just before the injection manifold (MFC1) so that the product of the concentration and flow rate is the desired pure component flow rate. During growth however, the mass flow controller set point is not adjusted. Consequently, concentration disturbances with time constants faster than a growth period can corrupt the target composition and thickness.

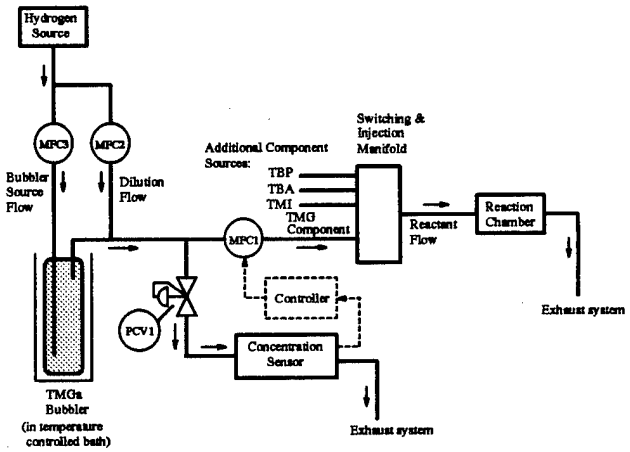

Fig. 1. Overview of the MOCVD gas flow for one source

In Gaffney et al., (1995a,b), a bubbler disturbance was shown to corrupt the pure component flow rate during growth. Evidence of the bubbler disturbance is shown in Figure 2, which is a comparison of the power spectral densities for the ultrasonic sensor signal under two conditions. The solid line is a concentration measurement of TMG in hydrogen under typical growth conditions. The dashed line is a concentration measurement of hydrogen only, without flowing through the bubbler, and is used as an indication of the levels of sensor noise. As shown, the TMG signal has energy in the PSD that does not exist in the sensor noise signal and hence is evidence of a bubbler concentration disturbance.

2.2. *Preliminary Control System*

A control scheme was implemented and described in Gaffney (1995a,b) where the controller objectives are nominal pure component flow regulation and disturbance rejection, remembering that the pure component

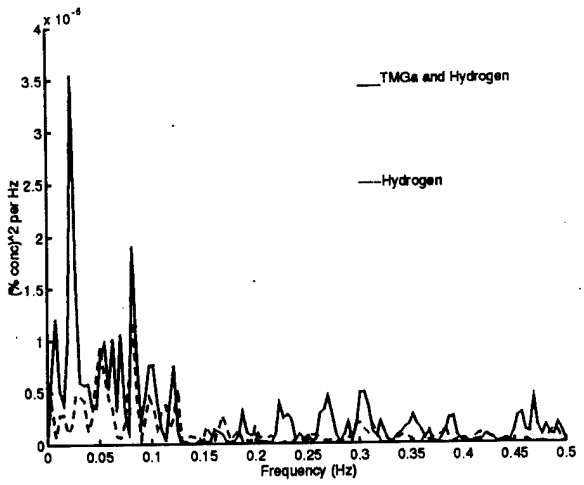

Fig. 2. Power spectral density of the ultrasonic concentration monitor signal, illustrating the low frequency energy found in a typical TMG measurement. For comparison, the sensor noise is shown by the dashed line.

flow is the product of component concentration and total flow. As shown in Figure 1, the controller input is the concentration monitor and the controller output dynamically adjusts the MFC1 set point. The preliminary controller structure consists of a low-pass filter and static inversion of the concentration signal. The inversion is simply a division of the optimal pure component flow rate (PCF_{opt}), as required for the proper growth, by the concentration signal (C_{meas}). The controller output, therefore, is a mass flow rate set point (F_{set}) that satisfies, $PCF_{opt} = C_{meas} \times F_{set}$.

2.3. *Closed Loop Experimental Results*

In order to evaluate the effectiveness of the composition controller, two alloy structures were grown using the same growth recipe. The first structure was grown under open loop conditions and the second under closed loop conditions. The structure grown consisted of alternating layers of InP (indium phosphide) and GaInAs, or more specifically, a 5-period $Ga_{0.47}In_{0.53}As$/InP (3000 Å/200 Å) superlattice. Further details of these test growths are described in Gaffney et al., (1995b). During both the open and closed loop growths, the TMG temperature bath was purposefully agitated, to cause a disturbance in the TMG concentration. The temperature of the TMG is nominally set at -10 degrees C. The agitation was such that the bath temperature was increased by 0.4 degrees C at the start of each InP layer. When the TMG was sent to the reactor for growth, the concentration had increased as a consequence of the warmer bath temperature. For these experiments, the desired composition is $Ga_{0.47}In_{0.53}As$. This corresponds to a desired TMG concentration of approximately 0.192 % by volume and a corresponding total flow rate of 90.57 sccm, or in other words, a pure component flow rate of 0.1739 sccm. However, because the temperature bath was increased by 0.4 degrees C before the growth of each consecutive GaInAs layer, the concentration and hence the corresponding pure component flow was corrupted. As a result, the desired composition was not obtained in the open loop growth as can be seen from the X-ray diffraction (XRD) results.

XRD techniques involve pointing a single wavelength X-ray source onto the sample at some incident angle and measuring the diffracted X-ray count. The sample is rocked through a range of incidence angles, while the X-ray count is measured, to generate a rocking curve. The key information occurs when the incidence angle is such that the diffracted X-rays undergo constructive interference and satisfy Bragg's law. If the desired structure grown was a ($Ga_xIn_{1-x}As$) layer on an InP substrate, one would expect two peaks, the first for the InP lattice and the second for the GaInAs lattice. The relative angle between the substrate and layer peaks is used in Bragg's law to determine the alloy molar breakdown x.

Figure 3 is a plot comparing the rocking curves of the open and closed loop growths. Recall that during these growths, the composition of the GaInAs layers were perturbed, via the temperature bath. In both plots, the InP (substrate) peak was purposefully centered at 0 arc seconds. The open loop plot contains one peak from the InP layers and five peaks from the GaInAs layers. Each GaInAs layer has a different composition, as is indicated by the five smeared peaks. The closed loop sample has only one peak from the five GaInAs layers indicating that the GaInAs layers all have the same composition (this substrate peak appears as two peaks in the figure because of corruption with the satellite fringes). From compositional analysis of these rocking curves, one can conclude that the open loop composition varied from $Ga_{0.479}In_{0.497}As$ to $Ga_{0.5}In_{0.5}As$, and the closed loop composition was maintained at $Ga_{0.473}In_{0.527}As$, in the presence of the concentration disturbance. Hence, composition control can improve the material quality in MOCVD processing.

3. MODEL OF MOCVD PROCESS

The challenge of improving composition precision in MOCVD processes has already been identified as an application for control (Stagg et al., 1992, Gaffney et al., 1995a,b). Now that a simple control implementation has been shown to be successful in improving the composition and thickness precision in III-V MOCVD,

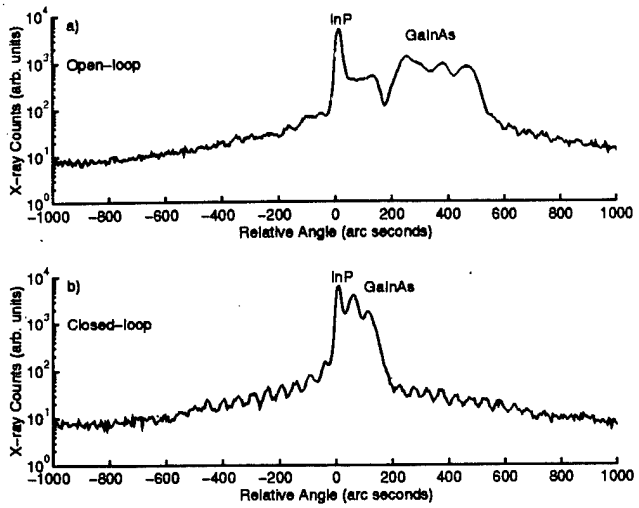

Fig. 3. X-ray diffraction rocking curves for (a) open and (b) closed loop growths during the TMG temperature bath agitation

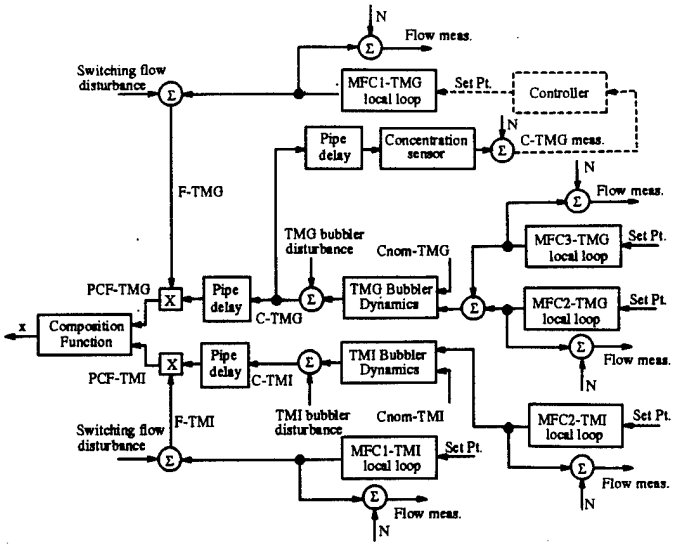

Fig. 4. MOCVD model diagram for control analysis

further control work first requires a system model. Complex models of the MOCVD process have been developed that capture three-dimensional transport phenomena, and detailed kinetic gas-phase and surface reactions (Jensen et al., 1991). Simulation of these types of models typically requires solving over 40,000 nonlinear algebraic equations that were generated from transforming partial differential equations and the corresponding boundary conditions. These models are used to predict the causes of growth rate variations, composition variations, and impurities. Additionally, models of this nature are extremely useful in the design of MOCVD reactors. For control analysis however, a simpler model that captures phenomena such as sensor noise, system bandwidths, and disturbance locations, will be more useful. Figure 4 is a system diagram of a model developed for control analysis. The model is not only used to design and test control laws, but is also useful when determining the optimal configuration of sensors and actuators for control. The model is based on the system shown in Figure 1 and illustrates the dynamics for two sources, TMG and TMI.

This modeling effort was developed to analyze the growth of the ternary compound $Ga_xIn_{1-x}As$, but can be extended to quaternary compounds, for example, and other other elements, such as $(Al_xGa_{1-x})_yIn_{1-y}P$. Because the growth is does not depend on the column V precursor delivery rate, only the TMG and TMI dynamics are included in the model. One goal of this model is to determine what factors will affect the composition x, in $Ga_xIn_{1-x}As$. Since the vapor concentration determines (to first order) the solid composition, the GaAs fraction in the resulting solid can be approximated by:

$$x = \frac{r_g(GaAs)}{r_g(InAs) + r_g(InAs)}, \tag{1}$$

assuming that GaAs and InAs are growing independently (Kuo et al., 1983). The growth rate of GaAs, r_g(GaAs), is a linear function of the pure component flow rate (or equivalently molar flow rate) of TMG, the column III source. And similarly, the growth rate of InAs, r_g(InAs), is a linear function of the pure component flow rate of TMI, another column III source. Because both growth rates are independent of the pure component flow rate of TBA, the column V source, Equation 1 can then be written as

$$x = \frac{k_1 f_{Ga}}{k_2 f_{In} + k_1 f_{Ga}} = \frac{f_{Ga}}{k f_{In} + f_{Ga}}, \tag{2}$$

where $k=k_1/k_2$ is a growth coefficient, f_{Ga} is the pure component flow rate of TMG, and f_{In} is the pure component flow rate of TMI (Kuo et al., 1983). The growth coefficient will vary according to growth conditions such as the susceptor temperature and the reactor pressure.

Consequently, the two inputs to the composition function in Figure 4 are the pure component flows of both TMG and TMI. The pure component flow of TMG is the product the hydrogen carrier and TMG (denoted F-TMG), multiplied with the concentration fraction of TMG in hydrogen (denoted C-TMG). This product is also shown in Figure 4. The total flow rate is controlled by MFC1-TMG. The MFC1 actuator local loop has been

identified with input-output data to be 1 Hz first-order lag from the set point input to the flow measurement output. As shown in the figure, the total flow from the actuator is corrupted by a switching flow disturbance, which typically occurs while growing layered structures that require multiple flow switches at the injection manifold (illustrated in Figure 1). The concentration of TMG in hydrogen is generated by flowing hydrogen through the bubbler as was described in a Section 2.1. This system is modeled by including the dynamics of both the input (MFC3-TMG) and dilution (MFC2-TMG) mass flow controllers. They are both modeled as 2 Hz first-order lags, based on the MFC manufacturer calibration installation records. These linear models for all mass flow controllers will accurately approximate the transducer behavior when the flow remains in the linear range of operation. If the flow levels come to within five percent of either zero or maximum flow then the linear model approximation will break down. The inputs to the TMG bubbler dynamic model consist of the nominal TMG concentration (Cnom-TMG) as well as the flow rates of both the input and dilution mass flow controllers. The bubbler model relates the ratio of the pure component flow of TMG to the total flow, and hence is a nonlinear system. The key feature of the bubbler concentration model is that it is corrupted by a concentration disturbance. Evidence of this disturbance was illustrated in Figure 2. In the model, the concentration of TMG is delayed by approximately 2 seconds due to a pipe transport time, which was determined from pipe geometry and typical flow rates. The model for TMI is similar, except the pipe delay is approximately 1 second and the TMI system does not have a dilution mass flow controller.

The concentration signal is measured by an ultrasonic sensor. This monitor measures the speed of sound in a input binary gas mixture to determine the gas concentration (Stagg et al., 1992). The concentration sensor has the capacity to monitor only one gas at a time. TMG was chosen to be measured because the TMG bubbler shows evidence of generating disturbances that possess time constants faster than some growth times and therefore need to be sensed in real-time for compensation, as shown in Gaffney et al., (1995a,b). The ultrasonic concentration sensor is not in-line with the flow from the mass flow controller (MFC1), and thus will feed back delayed information. From pipe volumes and flow rates, the concentration reading was determined to be lagging behind the MFC1 flow rate measurement by approximately 2 seconds. In addition, from input-output tests and discussions with the manufacturer (Grantham 1994), the bandwidth of the sensor is roughly 0.2 Hz and was modeled accordingly. For the simulations, all actuator and sensor outputs were clipped at the appropriate dynamic ranges, and sensor noises (N) were injected when required to investigate the consequences of closing a loop. The control system, that successfully improved both composition and thickness precision (Gaffney et al., (1995a,b)), is also included in the model. As illustrated in Figure 4, the control input is the concentration measurement of TMG and the output is the set point to the TMG mass flow controller (MFC1-TMG). The controller consisted of a 0.5 Hz 2 pole butterworth filter followed by the concentration inversion law, discussed in Section 2.2

The model was tested by simulating the open and closed loop runs of the perturbed GaInAs growths. The corresponding post-growth X-ray diffraction curves are shown in Figure 3 and will be used to compare the composition results. The simulations were performed by injecting the recorded time histories of the TMG bubbler disturbance (as measured by the concentration monitor). The TMI bubbler disturbance was not measured and hence not simulated. Any existing switching flow disturbances were not recorded nor simulated. For the open loop simulations, the recorded time history of the mass flow actuator command at MFC1-TMG was used to drive the set point. For the closed loop simulations, the model of the controller drove the MFC1-TMG set point based on the injected TMG bubbler disturbance. The set points for the remaining TMG mass flow controllers and all TMI mass flow controllers were constants that corresponded to the values coded in the run program. Before the open loop simulation was investigated, the growth coefficient (k in Equation 2) was determined using the composition and pure component flow information from an open loop calibration run. This calibration run was performed on the same day, under similar growth conditions, but without the purposefully inflicted concentration disturbance. The growth coefficient for the open loop growth was determined using the X-ray diffraction composition estimate, x = 0.477, and the pure component flow estimates, f_{Ga} = 0.1908% (from the concentration signal) × 90.58 sccm (from MFC1-TMG flow sensor) = 0.1728 sccm and f_{In} = 0.108% (estimate from earlier concentration measurement) × 194 sccm (from MFC1-TMI desired set point input) = 0.2085 sccm. The resulting growth coefficient is k = 0.905.

The composition time history for the open loop simulation is shown in Figure 5(a). The shaded areas in the figure correspond to times when the $Ga_xIn_{1-x}As$ layers are growing. During the remaining times, either InP layers are growing or a blanket of TBP (tertiarybutylphosphine) is flowing over the crystalline structure. The mean (simulated) composition, $\bar{x}$, for each of the

five $Ga_xIn_{1-x}As$ layers, are summarized in Table 1 and compared to the composition estimates from the X-ray diffraction testing. Excellent agreement is observed between the simulated and measured compositions.

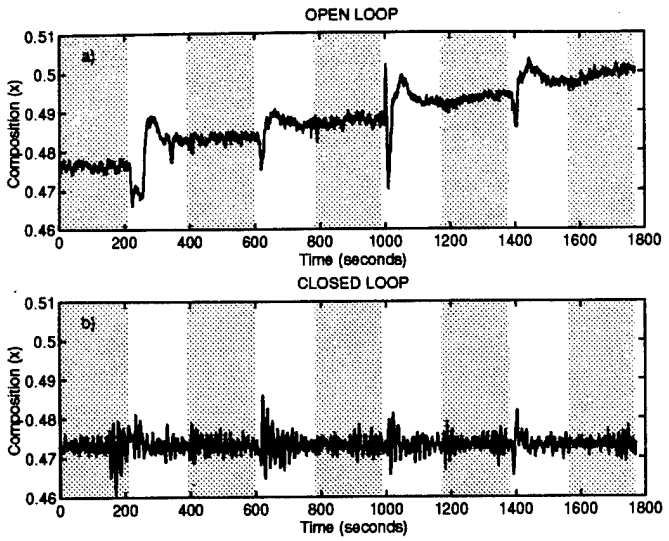

Fig. 5. Simulation of GaInAs composition for the (a) open loop and (b) closed loop growths.

Table 1 Comparison of the X-ray diffraction composition measurements (Meas.) with the simulated mean composition estimates (Sim.) for each of the five layers in the GaInAs open loop growth. *Note that it was not possible to accurately determine the composition of the second and third layers using X-ray diffraction techniques because the corresponding peaks are corrupted by the convolution with each other (cf., Figure 3).

Layer	1	2	3	4	5
Meas.	0.479	0.485*	0.485*	0.492	0.497
Sim.	0.477	0.483	0.487	0.493	0.499

For the closed loop simulation, the growth coefficient (k) was determined to be k = 0.917 by a closed loop calibration run, in a similar manner to the open loop procedure. For the closed loop calibration run, $f_{Ga} = 0.191\% \times 89.66$ sccm $= 0.171$ sccm, and $f_{In} = 0.108\% \times 194$ sccm $= 0.2095$ sccm. The resulting time history for the simulated composition in the closed loop experiment is shown in Figure 5. The mean (simulated) composition, $\bar{x} = 0.473$ for all the layers. The corresponding X-ray diffraction composition estimate is $x = 0.473$. This perfect agreement supports the claims and assumptions used to derive the model. The model can now be used to test other control schemes as is discussed in the next section.

4. CONCLUSIONS AND FUTURE WORK

The composition and thickness precision has be shown to improve using a relatively simple controller structure. Greater growth parameter control requires analysis with a system model. Although detailed models of the MOCVD process exist, a less complex model, tailored to a control framework is more useful when analyzing the application of control. The model developed herein captures the necessary process dynamics in mass transport and reaction kinetics and includes descriptions of both actuator and sensor bandwidths. The model has been shown to accurately estimate the composition of a ternary III-V compound semiconductor.

The MOCVD system model will be useful in testing controller stability robustness and performance via simulation, as the process dynamics are highly nonlinear. Additionally, the model was designed to examine different actuator/sensor configurations. Decisions regarding new sensor technologies, as well as what loops to close given a choice of actuators, will be investigated.

5. REFERENCES

Agrawal, G.P. and N. K. Dutta (1993). *Semiconductor Lasers.* Van Nostrand Reinhold, New York, 2nd edition.

Bastard, G. (1983). *Appl. Phys. Lett.*, **43**, 591.

Biefeld, R.M and S. R. Kurtz (1995). presented at the Seventh Biennial Workshop on Organometallic Vapor Phase Epitaxy, submitted to the Journal of Electronic Materials.

Blondelle, J., H. De Neve, P. Demeester, P. Van Daele, G. Borghs, and R. Baets (1995). *Electronics Letters*, **31**, 1286.

Dupuis, R.D. (1984) *Science*, bf 226, 623.

Gaffney, M.S., R. S. Smith, A. L. Holmes, Jr., C. M. Reaves, and S. P. DenBaars (1995a). *Proc. IEEE CDC.* p. 2490.

Gaffney, M.S, Casper M. Reaves, Roy S. Smith, Archie L. Holmes, Jr., and Steven P. DenBaars (1995). J. of Crystal Growth, revisions submitted.

Grantham, T. (1994). private communication.

Jensen, K.F., D. I. Fotiadis, and T. J. Mountziaris (1991). *J. Crystal Growth*, **107**, 1.

Kobayashi, N (1994). *J. Crystal Growth*, **145**, 1.

Kuo, C.P., R. M. Cohen, and G. B. Stringfellow (1983). *J. Crystal Growth*, **64**, 461.

Stagg, J.P., J. Christer, E.J. Thrush, and J. Crawley (1992). *J. Crystal Growth*, **120**, 98.